Supporting Information

Analogues Copper Nanoclusters ($Cu_{16/17}$) with Two Electron Superatomic and Mixed Valence Copper(II)/Copper(I) and Copper(I)/Copper(0) Characters

Shibaditya Kumar,[a] Saikat Mishra,[a] Aniruddha Das,[a] Kuldeep Mahiya,[b] Sourav Laha,[a] Milan Maji,[a] and Apurba K. Patra*[a]

[a]Department of Chemistry, National Institute of Technology Durgapur, Durgapur 713 209 (WB), India.

[b]Department of Chemistry, F. G. M. Government College, Adampur, Hisar-125052, Haryana, India.

Table of Contents

Experimental Section:

Materials and Reagents

The reagents such as thiophene-2-carbaldehyde, 3-methyl-2-thiophenecarbaldehyde, 2-amino-4-(trifluoromethyl)benzenethiol hydrochloride, $[Cu(CH_3CN)_4]PF_6$, $[Cu(CH_3CN)_4]ClO_4$, [*n*-Bu_4N][ClO_4] were purchased from Aldrich Chemical Co. and used without further purification. CH_3CN, CH_3OH, dimethylformamide (DMF), toluene, CH_2Cl_2, $CHCl_3$, diethyl ether (Et_2O) used either for spectroscopic studies or for syntheses were purified and dried following standard procedures prior to use.

Synthesis safety note: *Transition metal perchlorates are hazardous and explosive upon heating, should be handled cautiously*. [1] *No explosion occurred in the present study.*

Physical Measurements

The FTIR spectra of the ligands and their complexes were recorded on a Shimadzu IRAffinity-1S FT-IR spectrometer using ATR mode and KBr pellet in the range 4000 – 400 cm^{-1}. The UV-Vis and Vis-NIR absorption spectra were recorded respectively on an Agilent 8453 diode array spectrophotometer and Agilent Cary 5000 spectrophotometer. Elemental analyses were carried out on a Perkin-Elmer 2400 series-II CHNS analyser. The X-ray photoelectron spectroscopy (XPS) was performed on Omicron Nanotech instrument using monochromatic AlK_α radiation ($h\nu$ = 1486.7 eV). Binding energies were referenced to the C 1s peak at 284.6 eV. For Energy Dispersive X-ray analysis (EDS), Ametek EDAX detector attached with the FESEM was used. The Electron paramagnetic resonance (EPR) spectrum was obtained using MiniScope MS 5000 Magenttech EPR spectrometer at 77 K. The ESI-Mass spectra were recorded on Waters-HAB213 spectrometer or Water XEVO G2-XS QTOF spectrometer. The ^1H NMR spectra were recorded on JEOL JNM-ECS 400S NMR Spectrometer. Redox potentials were measured using CHI 1120A potentiometer using a three-electrode cell set up such as platinum, saturated calomel electrode (SCE) and a platinum wire as a working, reference and auxiliary electrode respectively. For constant potential electrolysis experiment under inert atmosphere, platinum mesh working electrode was used and a solute concentration of ~ (1×10^{-4}) - (5×10^{-5}) M was maintained.

X-ray Crystallography

Crystals of **1** suitable for X-ray diffraction, were grown by slow ether diffusion to the CH_3OH/Toluene (20:1 v/v) solution of the complex, while for the **2** crystals were grown by layering of toluene onto the CH_3OH/DMF/C_2H_5OH (2:1:0.1 v/v ratio) solution of the complex. In case of **3**, suitable crystal for X-ray diffraction was obtained by giving toluene layer on the top of the DMF/C_2H_5OH (30:1 v/v) solution of **1**. The intensity data for **1** (140 K), **2** (100 K) and **3** (150 K) were collected on a Bruker APEX-II CCD diffractometer with graphite monochromatized Mo/K_α radiation (for **2** and **3**) and Cu/K_α radiation (for **1**). Crystals of **1** and **2** are weak diffractor. These crystals of **2** and **1** diffract very weakly beyond 2θ = 37° and 88° which reflects in low and moderate $I/\sigma(I)$ value of 5.0 and 11.7 (mean signal to noise ratio) and in merging R value, R_{int} (16.14 % and 10.03%), respectively. So, the data was cut off at resolution 0.86 and 0.84 Å respectively for **1** and **2**. Crystal of **3** is a good diffractor and diffracts well upto 2θ = 50° ($I/\sigma(I)$ = 21.9, R_{int} = 6.40%). The data were corrected for Lorentz and polarization effects. Multi-scan absorption correction was applied. The structure was solved by direct methods using SHELXT[2] and refined by full-matrix least-squares refinement techniques on F^2, using SHELXL-2019/3.[3] All calculations were done with the help of OLEX2 crystallographic program.[4] For the molecular graphics, the program

OLEX2 and Mercury[5] were used. All non-hydrogen atoms were refined anisotropically except for some solvent molecules in the lattice. All hydrogen atoms were fixed geometrically with U_{iso} values of 1.2 times (for methylene and phenylene) and 1.5 times (methyl) the U_{iso} values of their respective carrier atoms. For **2**, the final residual indexes are; $R_1 = 0.1103$, $wR_2 = 0.2912$ for the observed and $R_1 = 0.2096$, $wR_2 = 0.3271$ for all reflections using 1293 parameters and 485 restraints. For **1**, the final residual indexes are; $R_1 = 0.0687$, $wR_2 = 0.1748$ for the observed and $R_1 = 0.1364$, $wR_2 = 0.2248$ for all reflections using 841 parameters and 273 restraints while for **3**, the final residual indexes are; $R_1 = 0.0554$, $wR_2 = 0.1437$ for the observed and $R_1 = 0.0767$, $wR_2 = 0.1587$ for all reflections using 965 parameters and 1080 restraints. The structure of **1** and **3** contains solvent accessible voids which generally occurs when the structure loses its long-range order when solvent molecules leave the crystal were calculated by Calculate Solvent Accessible Voids routine in Olex2. The structure of **3** have total solvent accessible volume/cell = 5335.5 $Å^3$ (15%) and radius (volume) of the largest spherical void is 3.60 Å (195.43 $Å^3$) and structure of **1** have total solvent accessible volume/cell = 12350.4 $Å^3$ (35%) and radius (volume) of the largest spherical void is 5.00 Å (523.60 $Å^3$). In **2**, total eight toluene molecules were located from the difference fourier map, out of which four are modelled while four are masked. A solvent mask was calculated and 760 electrons were found in a volume of 5234 $Å^3$ in 1 void per unit cell. This is consistent with the presence of 4[C_7H_8] per asymmetric unit which account for 800 electrons per unit cell. The detailed structure data for **1**-**3** are available at the Cambridge Crystallographic Data Centre with CCDC # 2363122-2363124 respectively.

Syntheses and Characterizations of ligands

2-(thiophen-2-yl)-5-(trifluoromethyl)benzothiazole, L4

A solution of 2-amino-4-(trifluoromethyl)benzenethiol (0.430 g, 2.229 mmol) in 10 ml of CH_3OH was added dropwise to a stirred solution of thiophene-2-carbaldehyde (0.250 g, 2.229 mmol) in 10 ml CH_3OH solution under Ar. Then the resulting solution was refluxed under Ar for 3h and CH_3OH was removed using a rotary evaporator. The yellow solid obtained was dissolved in 40 mL $CHCl_3$ and washed successively with distilled water then with brine solution and again with distilled water using separatory funnel. The $CHCl_3$ layer was taken in a conical flask and solid anhydrous Na_2SO_4 was added. After 2h the solution was filtered and the filtrate evaporated to dryness that yields yellow solid residue which was recrystallized from CH_3OH solution in air (0.492 g, yield: 77 %). Elemental analysis calculated for $C_{12}H_6F_3NS_2$ **(L4)**: C 50.52, H 2.12, N 4.91; Found: C 50.49, H 2.10, N 4.88; IR frequencies (KBr disk, cm^{-1}): 3105(w), 3080(w), 1605($\nu_{C=N}$, s), 1590(s), 1562(s), 1426(m), 1405(s), 1326(s), 1267(w), 1237(w) 1160(s), 1138(s), 1110(s), 1076(s), 1042(m), 951(w), 917(s), 880(m), 860(m), 823(w), 813(m), 776(m), 744(w), 714(s), 692(m), 652(m), 561(m), 495(m) 478(w); ^{1}H NMR (400 MHz, $CDCl_3$) δ_{ppm}: 8.67 (1H, s, Ph proton ortho to imine-N), 7.72 (1H, d, J = 4 Hz, Ph proton meta to $–CF_3$ group), 7.63 (2H, t, J = 4 Hz, proton ortho to $–CF_3$ group and at no 3 with respect to thiophene-S), 7.40 (1H, dd, J = 8 Hz, at no 5 w.r.t thiophene-S), 7.20 (1H, t, J = 4 Hz, at no 4 w.r.t thiophene-S); ^{13}C NMR (100MHz, $CDCl_3$) δ_{ppm} : 162.81, 153.94, 139.64, 133.30, 132.53, 132.28, 131.60, 131.40, 128.39, 125.30, 122.69, 122.04; ESI mass: m/z (%) = 285.995 (100) $\{M+H\}^+$.

2-(3-methylthiophen-2-yl)-5-(trifluoromethyl)benzothiazole, ^{Me}L4

To a solution of 3-methylthiophene-2-carbaldehyde (0.200 g, 1.585 mmol) in 15 mL of dry CH_3OH was added a methanol solution (10 mL) of 2-amino-4-(trifluoromethyl)benzenethiol (0.306 g, 1.585 mmol) under Ar. The resulting reaction mixture was then refluxed under Ar for 4 h. Next the solvent was removed that afforded a reddish yellow solid. This solid was dissolved in 30 mL of $CHCl_3$ and washed successively with distilled water, brine solution and finally with

distilled water. The organic layer separated was then dried over anhydrous Na_2SO_4, filtered and solvent was removed completely resulting a yellow solid. (0.382 g, 1.27 mmol, yield = 80%). Elemental analysis calculated for $C_{13}H_8F_3NS_2$ **(^{Me}L4)**: C 52.17, H 2.69, N 4.68; Found: C 52.15, H 2.66, N 4.63 ; IR frequencies (KBr disk, cm^{-1}): 3097(w), 2926(w), 2854(w), 1608($\nu_{C=N}$, s), 1588(s), 1564(m), 1399(s), 1324(vs), 1250(m), 1169(m), 1135(s), 1114(m), 1080(s), 1045(w), 896(m), 820(m), 768(w), 730(m), 700(w), 670(w), 652(w), 534(w), 486(w); ^{1}H NMR (400 MHz, $CDCl_3$) δppm: 8.64(1H, s, Ph proton ortho to imine-N), 7.66(1H, d, J = 8 Hz, Ph proton meta to $–CF_3$ group), 7.49(1H, d, J = 4 Hz, Ph ring proton ortho to $–CF_3$ group), 7.34(1H, d, J = 8 Hz, at no 5 w.r.t thiophene-S), 6.95(1H, d, J = 4 Hz, at no 4 w.r.t thiophene-S), 2.53(3H, s, methyl group proton); ^{13}C NMR (100MHz, $CDCl_3$) δ_{ppm} : 152.99, 149.01, 144.17, 136.33, 136.03, 131.56, 131.43, 129.52, 125.97, 123.10, 122.70, 114.09, 14.52; ESI mass: m/z (%) = 300.006 (100) $\{M+H\}^+$.

Syntheses and Characterizations of Complexes

$[(L4)_{12}Cu^{I}_{15}Cu^{II}(\mu_4\text{-}S)](PF_6)_3$, 1

Method A: To a degassed solution of thiophene-2-carbaldehyde (0.150 g, 1.330 mmol) in 10 mL of dry degassed CH_3OH was added a degassed CH_3OH solution (5 mL) of 2-amino-4-(trifluoromethyl)benzenethiol (0.258 g, 1.330 mmol). The resulting reaction mixture was then refluxed under Ar for 2 h. To this solution was added solid $[Cu(CH_3CN)_4]PF_6$ (0.495 g, 1.33 mmol) that developed immediately a deep red clean solution which was further refluxed for 1 h. After cooling the solution to room temperature, dry degassed ether was layered on top of this reaction mixture and kept at -35 °C freezer for a day. The deep red precipitate formed was collected by filtration. Slow ether diffusion to the CH_3OH-Toluene (20:1 v/v) solution of this red solid afforded dark red crystal of **1** (0.331 g, yield: 70 % based on Cu). IR frequencies (KBr disk, cm^{-1}): 3435(w), 3105(w), 1600($\nu_{C=N}$, m), 1576(s), 1556(m), 1418(m), 1400(s), 1326(s), 1272(m), 1172(m), 1127(s), 1088(s), 923(m), 840($\nu_{PF6\text{-}}$, s), 856(w), 790(w), 716(m), 558(ν_{PF6^-}, s), 487(m); Elemental analysis calcd for $C_{144}H_{84}Cu_{16}F_{54}N_{12}P_3S_{25}$, **1**: C 35.16, H 1.72, N 3.42. Found: C 35.02, H 1.70, N 3.35; ESI MS: m/z = 634.84 $[(L4)_2Cu]^+$, 762.67 $[(L4)_2Cu_3]^+$, 1111.56 $[(L4)_3Cu_4]^+$, 1462.44 $[(L4)_4Cu_5]^+$, 1811.33 $[(L4)_5Cu_6]^+$, 1900.24 $[(L4)_5Cu_6+CH_3OH+H_2O+K]^+$, 2162.17 $[(L4)_6Cu_7]^+$; UV/Vis in CH_3CN, λ_{max}(ε in $M^{-1}cm^{-1}$): 275(166375), 325(148030), 485(23350), 720(4281), 845(3622); Vis/NIR in CH_3CN, λ_{max}(ε in $M^{-1}cm^{-1}$): 485(23350), 720(4281), 845(3622), 1040 (4690), 1040 (4690), 1185(11238), 1700(25614); Vis/NIR in DMF, λ_{max}(ε in $M^{-1}cm^{-1}$): 485(23405), 720(5227), 845(4675), 1040 (4720), 1185(12990), 1700(28590); Vis/NIR in DMSO, λ_{max}(ε in $M^{-1}cm^{-1}$): 485(23495), 720(5723), 850(5175), 1040 (4780), 1185(14270), 1700(30735).

Method B: Ligand **L4** (0.300 g, 1.051 mmol) was dissolved in 25 ml of dry degassed CH_3OH. To this solution, solid $[Cu(CH_3CN)_4](PF_6)$ (0.391 g, 1.051 mmol) was added under Ar that results a dark red solution. The solution was refluxed for 2h under inert atmosphere. After cooling down to room temperature, the dark red solution was concentrated using rotary evaporator. Dry degassed ether layering on top of this solution resulted deep red precipitate after a day at 4 ^{0}C temperature. The red solid was then dissolved in MeOH-Toluene (20:1 v/v) and kept under slow diffusion of diethyl ether at 4^{0}C. After 7days dark red block-shaped crystals of **1** were found those are suitable for X-ray diffraction (0.383 g, yield: 81 % based on Cu).

Method C: To a dry DMF solution (4mL) of **3** (0.1g, 0.0190 mmol) was added solid sodium sulfide (0.0026g, 0.0285 mmol). The mixture was stirred at room temperature for 12 hours under aerobic condition. Some black precipitates were found with the dark red solution. The solution was then collected by filtration and the solvent was evaporated to dryness

under reduced pressure. Then the red crude solid obtained was dissolved in CH_3OH/Toluene mixed solvent (20:1 v/v) and kept for diethyl ether diffusion at 4^0C. After 5 days dark red crystals of **1** (0.065g, yield: 69%) were obtained.

$[(^{Me}L4)_{12}Cu^{I}_{15}Cu^{0}(\mu_4\text{-}S)]ClO_4 \bullet 8C_7H_8$, 2

Method A: The CH_3OH solution (10 mL) of 2-amino-4-(trifluoromethyl)benzenethiol (0.306 g, 1.585 mmol) was added drop wise to a stirred degassed CH_3OH solution (10 mL) of 3-methylthiophene-2-carbaldehyde (0.200 g, 1.585 mmol) under Ar. The mixture was refluxed under Ar for 2 h resulting a light-yellow solution. To this solution was added solid $[Cu(CH_3CN)_4]ClO_4$ (0.518 g, 1.585 mmol) under Ar that generates deep red clean solution. At refluxing condition soon, the precipitation of reddish-brown compound was observed. The solution was refluxed further for 1 h and cooled to room temperature. The brown solid precipitated out was collected by filtration, washed with CH_3OH and diethyl ether and next dried under vacuum. Toluene layering over the solution of brown precipitate in CH_3OH/DMF/C_2H_5OH (2:1:0.1 v/v ratio) mixed solvent afforded brown needle-shaped crystals of **2** suitable for X-ray diffraction (0.323 g, yield: 65 % based on Cu). IR frequencies (KBr disk, cm^{-1}): 3091(w), 2926(w), 1598($\nu_{C=N}$, m), 1575(s), 1556(s), 1397(s), 1326(vs), 1270(w), 1256(w), 1171(m), 1121(m), 1090(ν_{ClO4^-}, vs), 952(w), 907(m), 828(w), 785(w), 731(m), 623(ν_{ClO4^-}, m), 482(m); Elemental analysis calcd for $C_{212}H_{172}ClCu_{16}F_{36}N_{12}O_4S_{25}$, **2**: C 46.39, H 3.16, N 3.06. Found: C 45.90, H 3.09, N 3.04; ESI MS: m/z = 1153.71 $[(^{Me}L4)_3Cu_4]^+$, 1518.63 $[(^{Me}L4)_4Cu_5]^+$, 1881.57 $[(^{Me}L4)_5Cu_6]^+$, 1981.47 $[(^{Me}L4)_5Cu_7+CH_3OH+3H]^+$, 4694.93 $\{[(^{Me}L4)_{12}Cu_{16}(\mu_4\text{-}S)]+H_2O+H+Na\}^+$; UV/Vis in CH_3CN, λ_{max}(ε in $M^{-1}cm^{-1}$): 310(107450), 330(sh, 105300), 476(21160); Vis/NIR in CH_3CN, λ_{max}(ε in $M^{-1}cm^{-1}$): 476(21160); Vis/NIR in DMF, λ_{max}(ε in $M^{-1}cm^{-1}$): 476(22125); Vis/NIR in DMSO, λ_{max}(ε in $M^{-1}cm^{-1}$): 476(21638).

Method B: To a stirred reddish yellow solution of ligand **^{Me}L4** (0.300 g, 1.002 mmol) in 30 ml dry degassed CH_3OH was added solid $[Cu(CH_3CN)_4]ClO_4$ (0.328 g, 1.002 mmol), resulting a dark red solution. The solution was refluxed for 1h. After cooling to room temperature, reddish brown solution was kept in refrigerator at 4ºC for overnight. Brown precipitate formed was collected by filtration. Toluene layering over the solution of reddish-brown solid in CH_3OH/DMF/C_2H_5OH (2:1:0.1 v/v ratio) mixed solvents afforded brown needle-shaped crystals of **2** suitable for X-ray diffraction (0.375 g, yield: 76 % based on Cu).

$[(L4)_{12}Cu^{I}_{15}Cu^{0}_2(DMF)](PF_6)_3 \bullet C_2H_5OH \bullet 2C_7H_8$, 3

Method A: Dark red DMF/C_2H_5OH (30:1 v/v) solution (2.5mL) of **1** (0.050g, 0.01016 mmol) was taken in a test tube, toluene was layered on it and kept undisturbed at room temperature in air. After 14 days, it afforded dark reddish brown block shaped crystals of **3** (0.015 g, yield: 28%), suitable for X- ray diffraction. IR frequencies (KBr disk, cm^{-1}): 3442(w), 3085(w), 1602($\nu_{C=N}$, m), 1577(s), 1557(m), 1418(m), 1400(s), 1327(s), 1272(m), 1172(m), 1124(s), 1088(s), 923(m), 840(ν_{PF6^-}, s), 856(w), 790(w), 734(m), 716(m), 558(ν_{PF6^-}, 3), 484(m); Elemental analysis calcd for $C_{163}H_{113}Cu_{17}F_{54}N_{13}O_2P_3S_{24}$, **3**: C 37.26, H 2.17, N 3.47. Found: C 37.18, H 2.13, N 3.45; ESI MS: m/z = 634.84 $[(L4)_2Cu]^+$, 985.87 $[(L4)_3Cu_2]^+$, 1048.64 $[(L4)_3Cu_3]^+$, 2797.18 $[(L4)_8Cu_8]^+$; UV/Vis in CH_3CN, λ_{max}(ε in $M^{-1}cm^{-1}$): 272(128990), 312(sh, 114830), 468(20690); Vis/NIR in DMF, λ_{max}(ε in $M^{-1}cm^{-1}$): 468(20700).

Method B: A dark red DMF solution (3mL) of **1** (0.060g, 0.0122 mmol) was stirred at 55^0C for 48 hours under aerobic condition. Some green precipitates were found with the dark red solution. The solution was then collected by filtration and dry diethyl ether layering on it afforded dark reddish-brown crystalline compound of **3** (0.017 g, yield: 26%) at 4 ^{0}C after two days.

Table S1: Data Collection and Structure Refinement Parameters for Complexes **1**, **2** and **3**

Complex	**1**	**2**	**3**
formulae	$C_{144}H_{84}Cu_{16}F_{54}N_{12}P_3S_{25}$	$C_{212}H_{172}ClCu_{16}F_{36}N_{12}O_4S_{25}$	$C_{163}H_{113}Cu_{17}F_{54}N_{13}O_2P_3S_{24}$
Formula wt.	4919.28	5489.20	5254.19
crystal system	trigonal	monoclinic	trigonal
Colour	Red	brown	brown
Space group	R3c	C2/c	R3c
a (Å)	24.8150(6)	39.487(9)	24.8645(11)
b (Å)	24.8150(6)	20.216(3)	24.8645(11)
c (Å)	66.157(3)	31.428(5)	66.598(6)
α (º)	90	90	90
β (º)	90	113.044(7)	90
γ (º)	120	90	120
V (Å^3)	35280(2)	23086(7)	35657(4)
Z	6	4	6
d_{calc}(g cm^{-3})	1.389	1.579	1.468
θ range, deg	4.009-63.403	2.206-24.999	2.460-24.998
μ (mm^{-1})	4.513	1.761	1.802
F(000)	14562	11060	15636
Reflections collected	71375	85171	95809
Data/restraints/ parameters	11546/273/841	20081/485/1293	13680/1080/965
R_1 [I>2σ(I)][a]	0.0687	0.1103	0.0554
wR_2 [I>2σ][b]	0.1748	0.2912	0.1437
GOF	0.984	1.028	1.103
res. dens. eÅ^{-3}	0.701/-0.922	1.585/-1.260	0.814/-1.685

[a] $R_1 = \sum||F_o| - |F_c||/\sum|F_o|$, [b] $wR_2 = \{\sum [w(F_o^2 - F_c^2)^2] / \sum w [(F_o^2)^2]\}^{1/2}$

Table S2: The Cu-Cu distance (Å) and the Cu-S-Cu angles (^{0}) of the two types of Cu_2S_2 squares of **1**-**3**

Complexes	$Cu_2(\mu\text{-}S)_2$ Square		$Cu(\mu\text{-}S)_2Cu^{Td}$ Square		
	Cu-Cu (Å)	Cu-S-Cu (^{0})	Cu-Cu^{Td} (Å)	Cu-S-Cu^{Td} (^{0})	Avg.Cu-N (Å)
1	3.188(5)-3.191(4)	78.9(2)-79.0(2)	2.657(4)-2.682(4)	63.2(2)-64.0(2) 70.6(2)-72.2(2)	1.98(2)
2	3.148(2)-3.223(3)	75.3(1)-81.0(1)	2.607(2)-2.732(3)	62.08(9)-65.2(1) 69.1(1)-72.9(1)	1.984(11)
3	3.145(2)-3.196(2)	77.4(1)-79.2(1)	2.637(2)-2.685(2)	62.72(8)-64.15(8) 69.96(9)-71.9(1)	1.990(8)

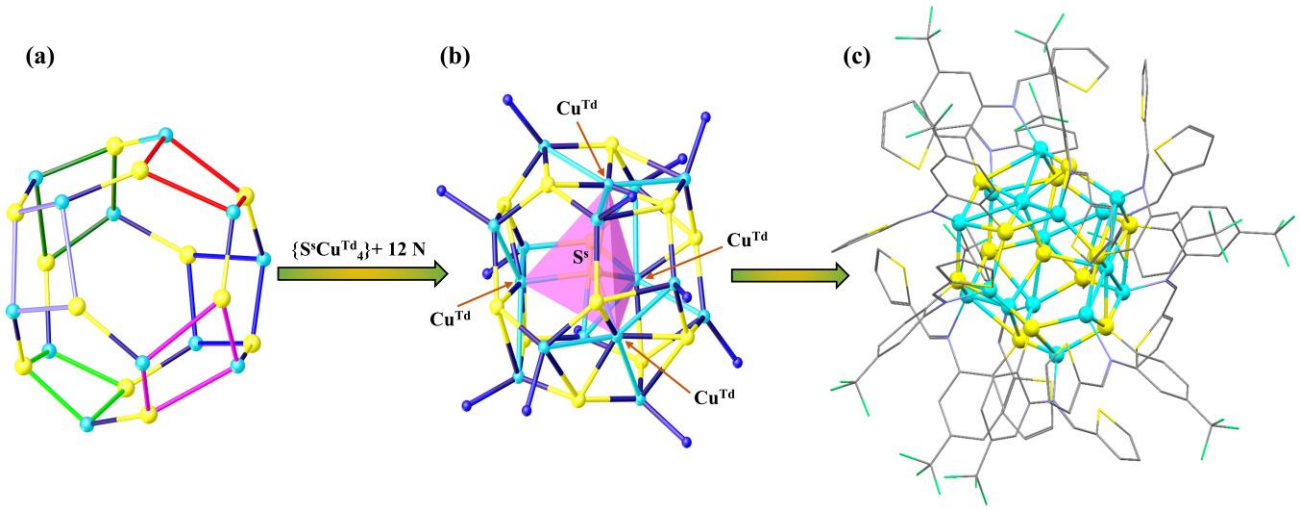

Figure S1: (a) Ball and stick diagram showing the $Cu_{12}S_{12}$ convex sphere-shaped shell of **1** and its six Cu_2S_2 square units, presented with red, blue, pink, light green, dark green and purple color. The Cu atoms are cyan and the S atoms are yellow; **(b)** the $\{S^sCu^{Td}_4\}$ tetrahedral core (pink) @$Cu_{12}S_{12}$ shell and 12 N of L4 for **1**, showing the coordination zone of all Cu and S atoms; **(c)** the full view of the cationic part of **1** with the atoms linked to C and C atoms depicted in wire frame. The disordered F atoms of the -CF_3 groups, the hydrogen atoms and the counter anions are omitted for clarity.

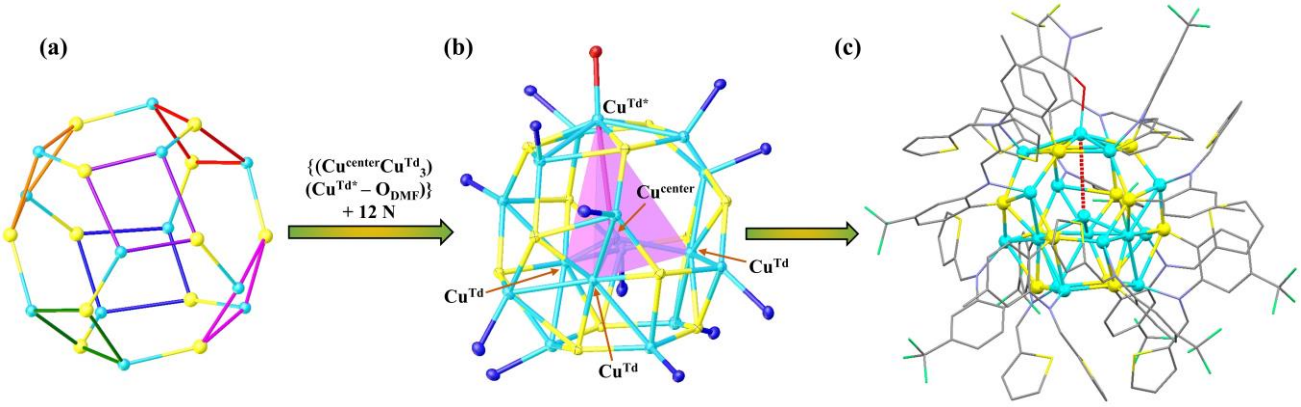

Figure S2: (a) Ball and stick diagram showing the $Cu_{12}S_{12}$ convex sphere-shaped shell of **3** and its six Cu_2S_2 square units, presented with red, blue, pink, green, purple and orange color. The Cu atoms are cyan and the S atoms are yellow; **(b)** the trigonal pyramidal $\{(Cu^{center})Cu^{Td}_3\}$ core @$Cu_{13}S_{12}$ shell plus 12 N of L4 and the DMF 'O' atom of **3** showing coordination of each Cu and S atoms. The pink solid line depicts long Cu^{center}-Cu^{Td*} bond along C_3 axis; **(c)** the full view of the cationic part of **3** with the atoms linked to C and C atoms depicted in wire frame. The red dotted line indicates the long Cu^{center}-Cu^{Td*} bond. The disordered F atoms of the -CF_3 groups, the hydrogen atoms and the counter anions are omitted for clarity.

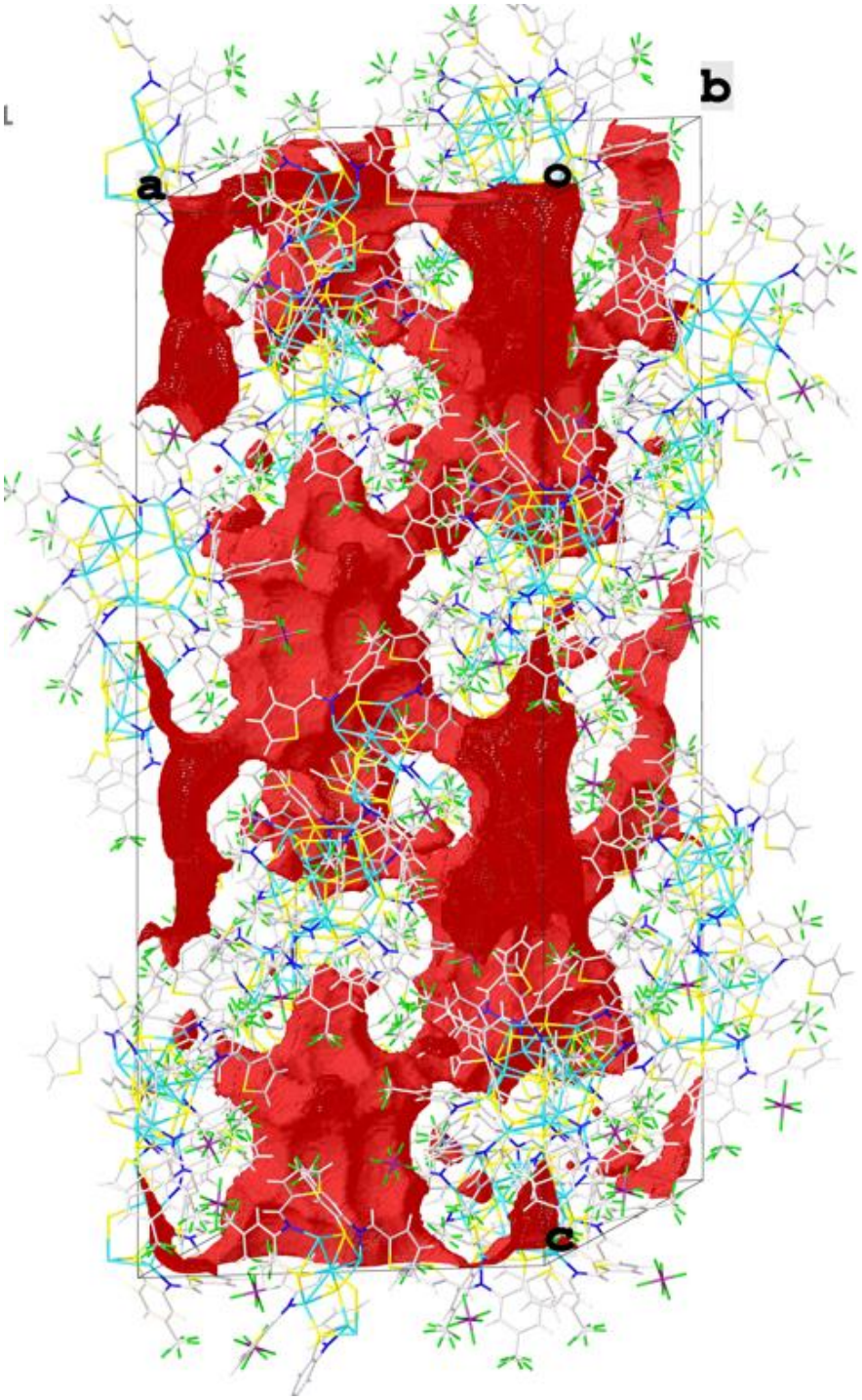

Figure S3: Solvent accessible voids (red surfaces) in **1**.

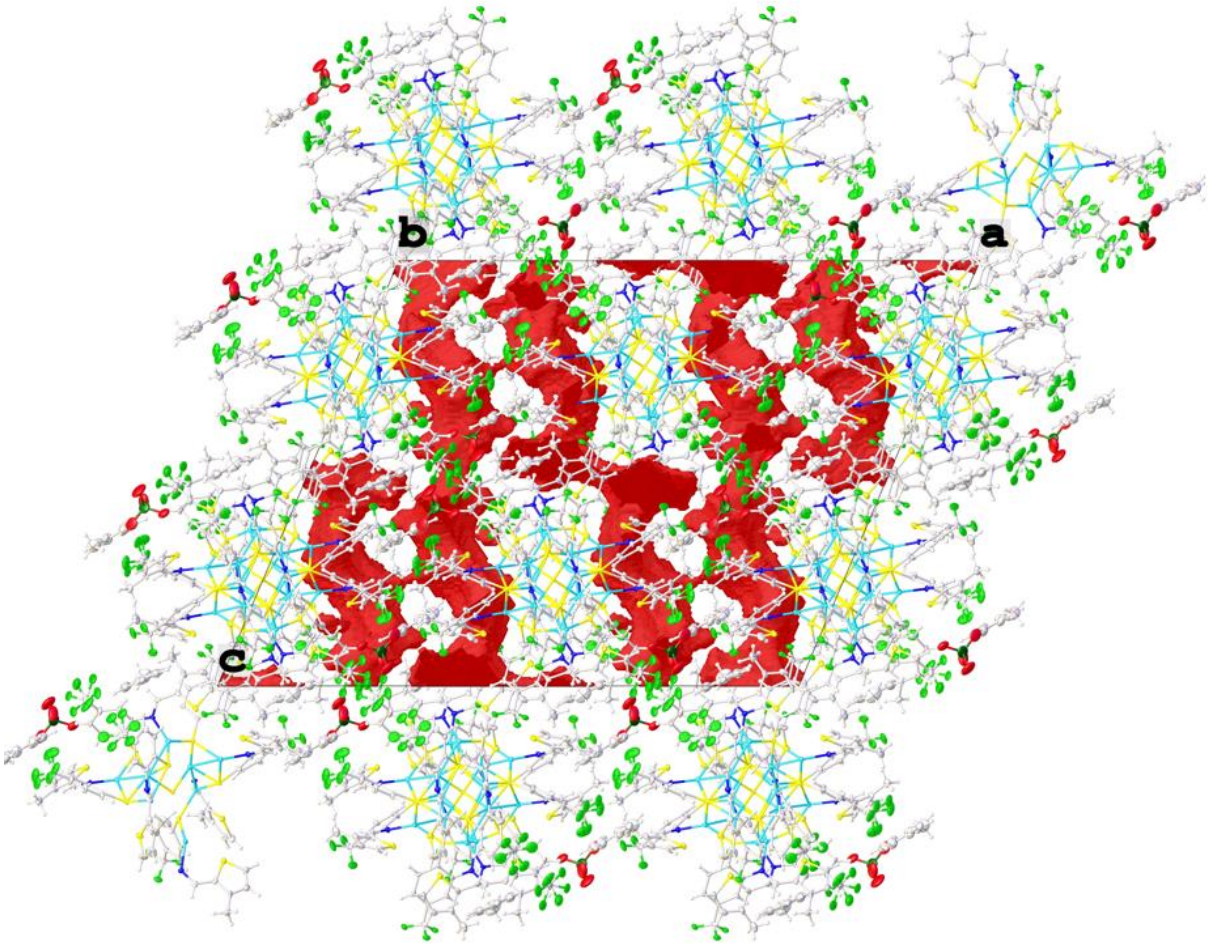

Figure S4: Solvent accessible voids (red surfaces) in **2**.

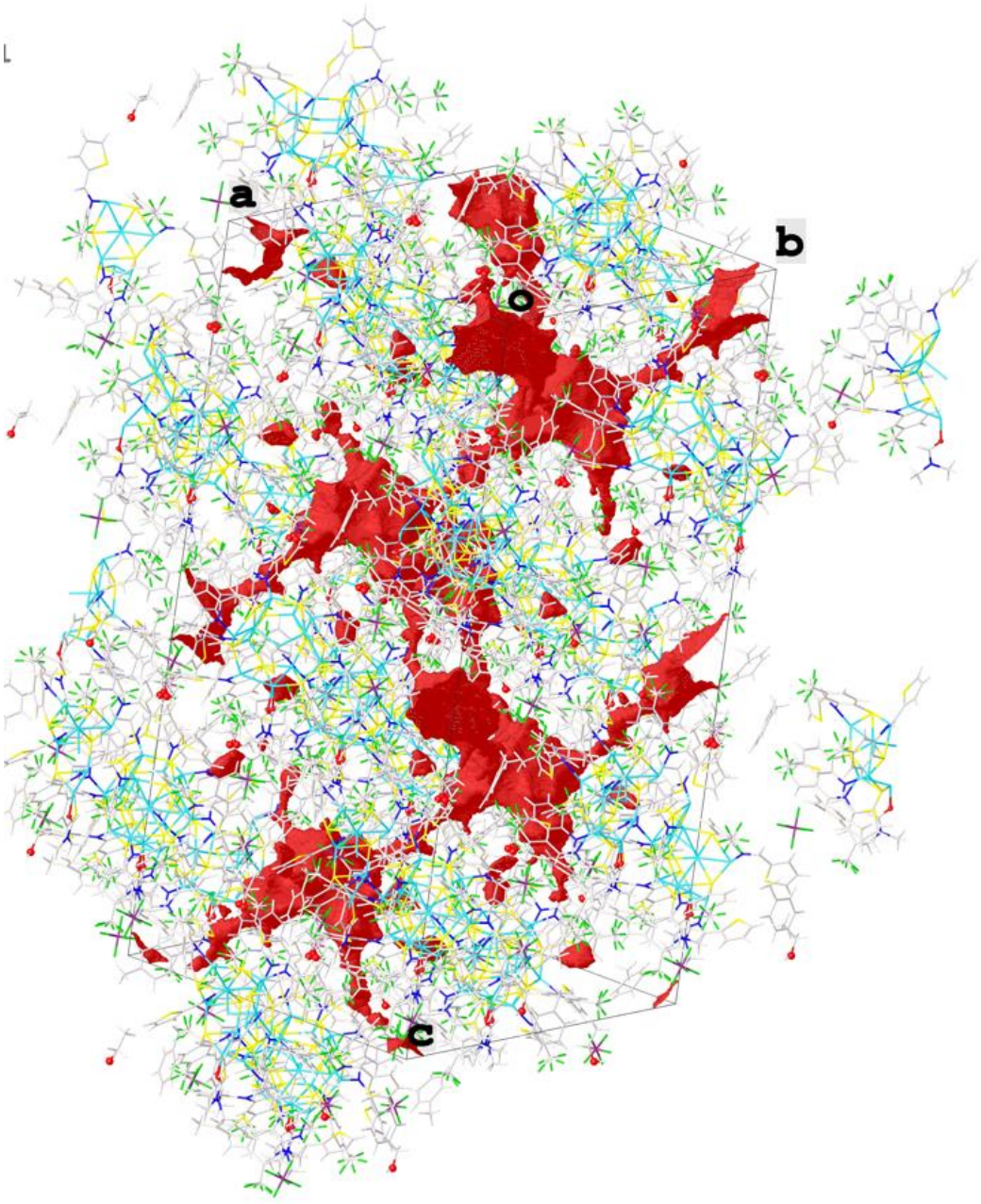

Figure S5: Solvent accessible voids (red surfaces) in **3**.

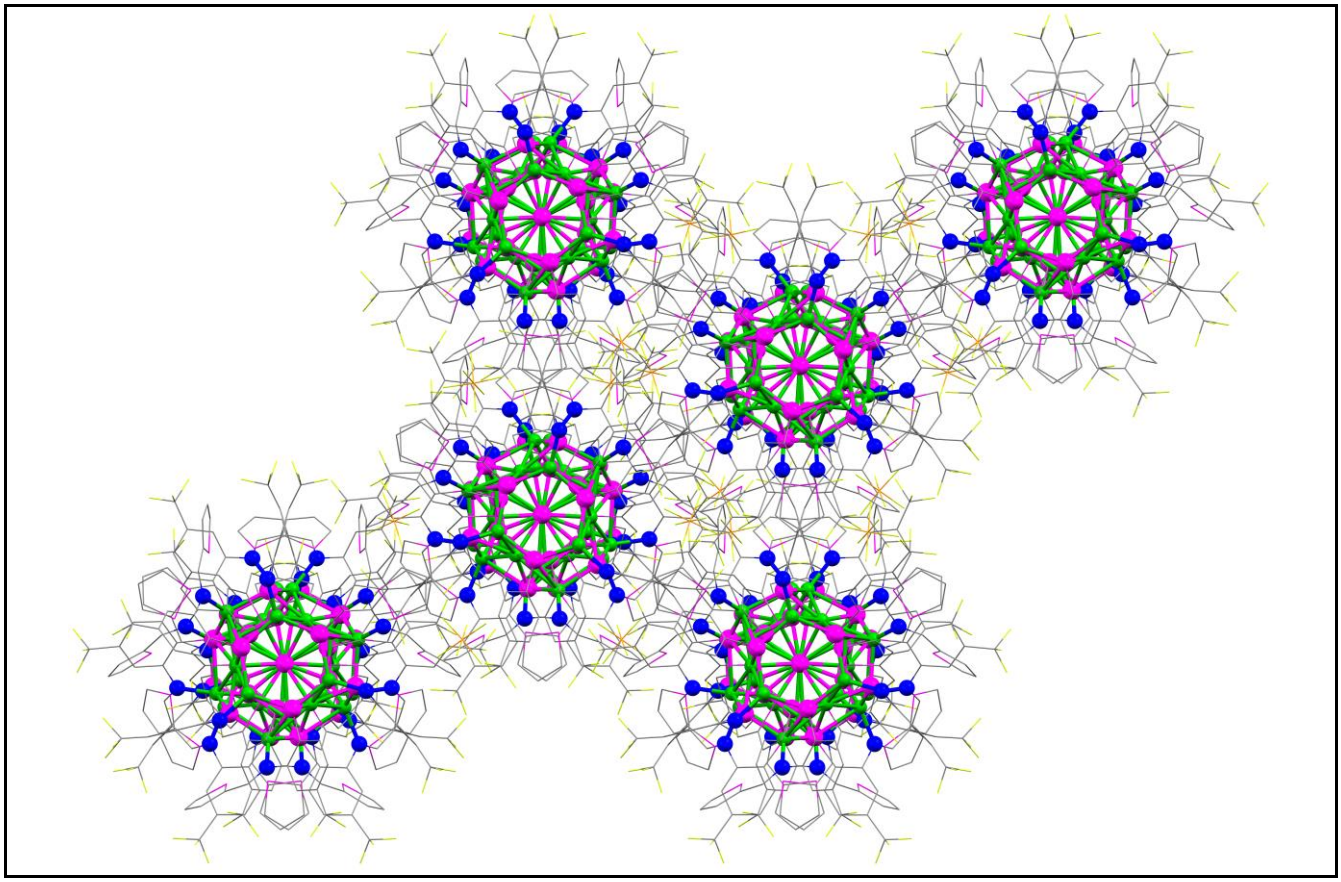

Figure S6: The crystal packing diagram of **1** depicting the $Cu_{12}S_{12}$ convex sphere-shaped shell, $\{S^sCu^{Td}{}_4\}$ tetrahedral core and the 12 N of L4 for **1** as ball and stick (copper atoms are green, sulphur atoms are purple and the nitrogen atoms are blue) and the remaining atoms as in wire frame. The disordered F atoms of $–CF_3$ groups and the H atoms are omitted for clarity. View along c axis.

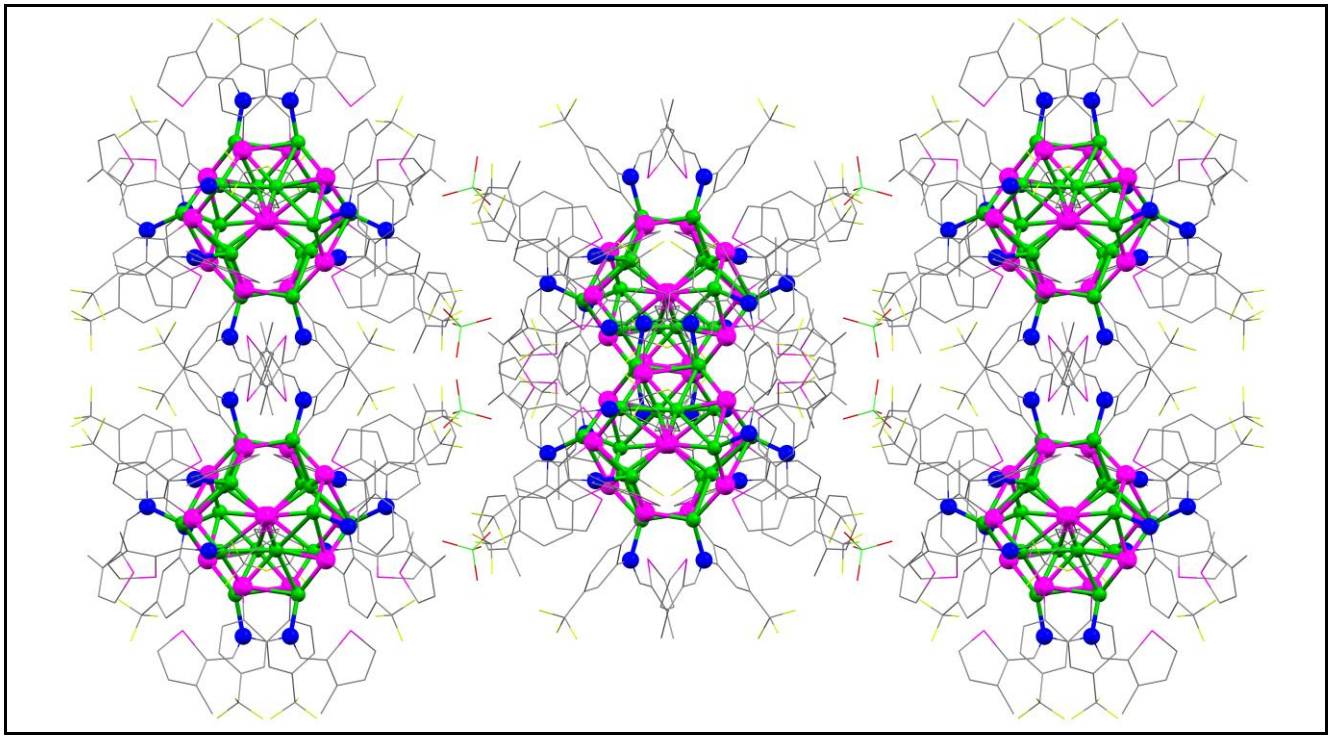

Figure S7: The crystal packing diagram of **2** depicting the $Cu_{12}S_{12}$ convex sphere-shaped shell, $\{S^sCu^{Td}_4\}$ tetrahedral core and the 12 N of ^{Me}L4 for **2** as ball and stick (copper atoms are green, sulphur atoms are purple and the nitrogen atoms are blue) and the remaining atoms as in wire frame. The disordered F atoms of $–CF_3$ groups and the H atoms are omitted for clarity. View along c axis.

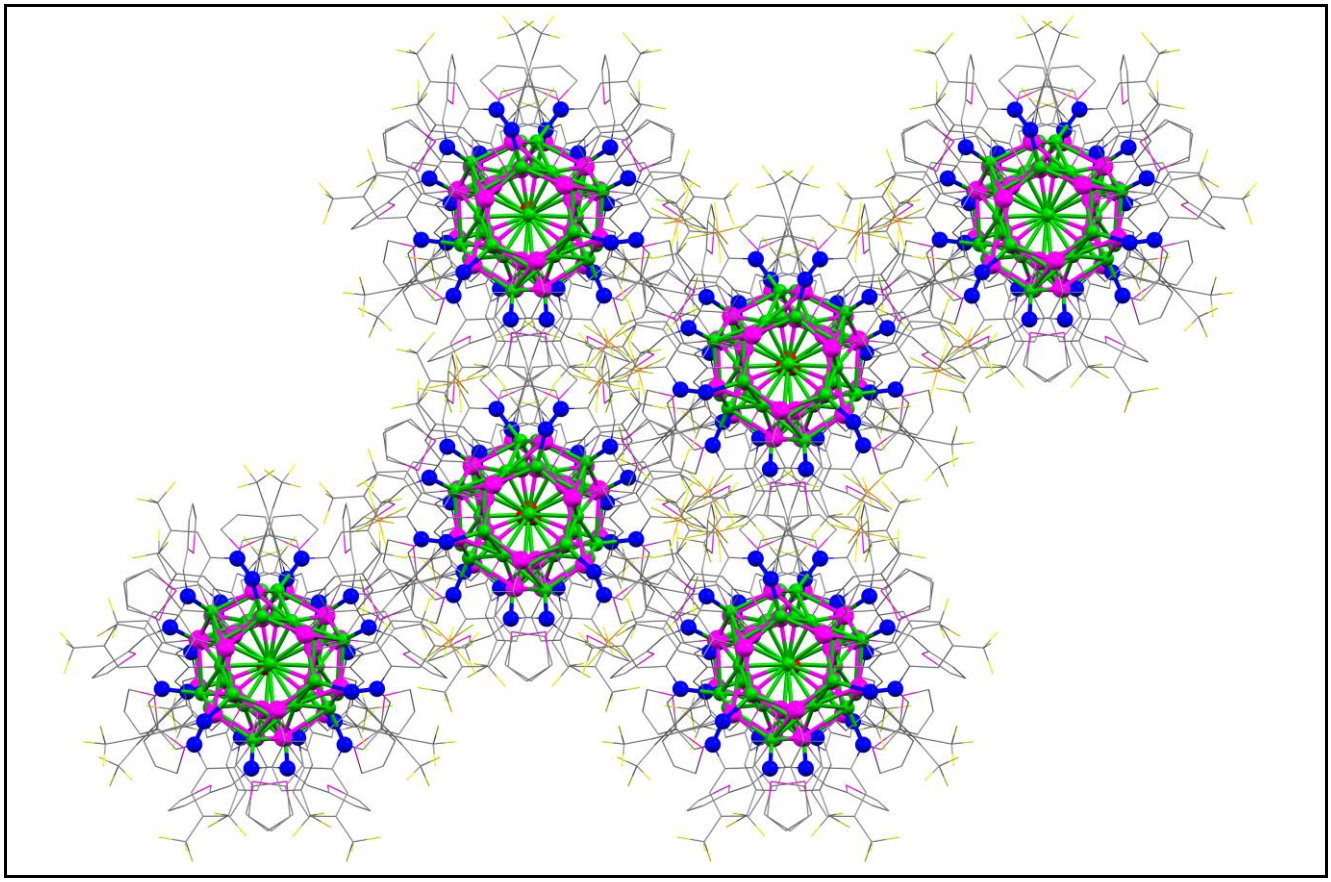

Figure S8: The crystal packing diagram of **3** depicting the $Cu_{13}S_{12}$ shell, $\{(Cu^{center})Cu^{Td}_3\}$ trigonal pyramidal core, O atom of coordinated DMF molecule and the 12 N of L4 for **3** as ball and stick (copper atoms are green, sulphur atoms are purple, nitrogen atoms are blue and the oxygen atoms are red) and the remaining atoms as in wire frame. The disordered F atoms of $–CF_3$ groups and the H atoms are omitted for clarity. View along c axis.

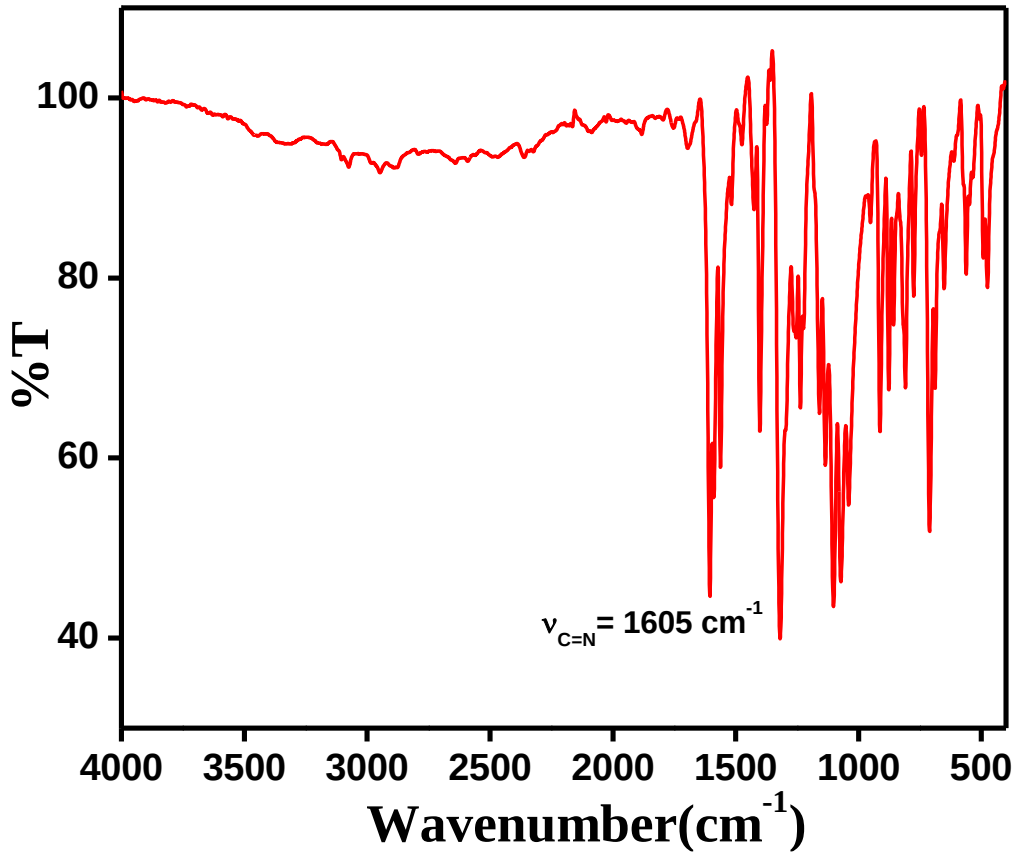

Figure S9: FTIR Spectrum of **L4** in KBr disk, in the range 4000-400 cm^{-1}.

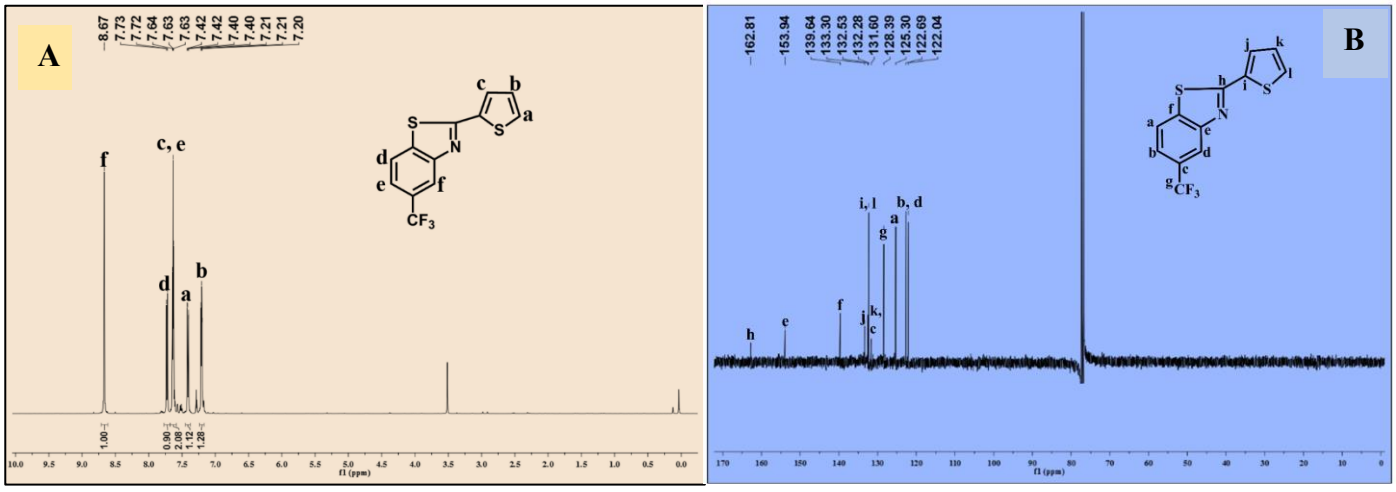

Figure S10: (A) ^{1}H NMR spectrum of **L4** in $CDCl_3$, **(B)** ^{13}C-NMR spectrum of **L4** in $CDCl_3$.

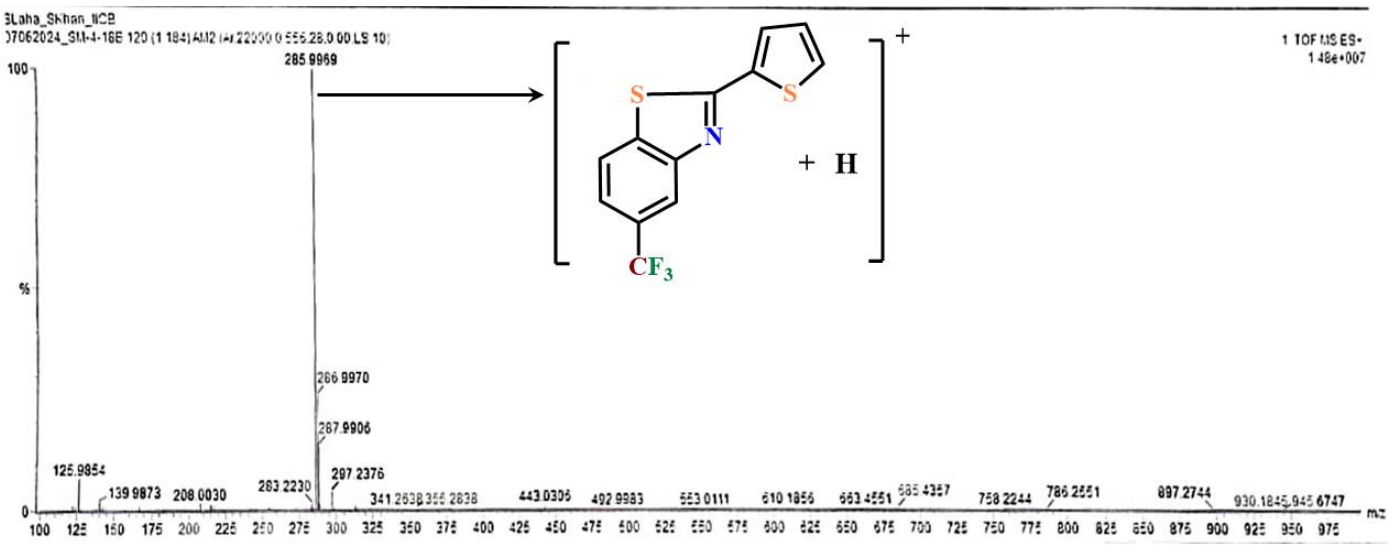

Figure S11: ESI mass spectrum of **L4** measured in CH_2Cl_2, peak at *m/z* = 285.995 corresponds to $\{M+H\}^+$.

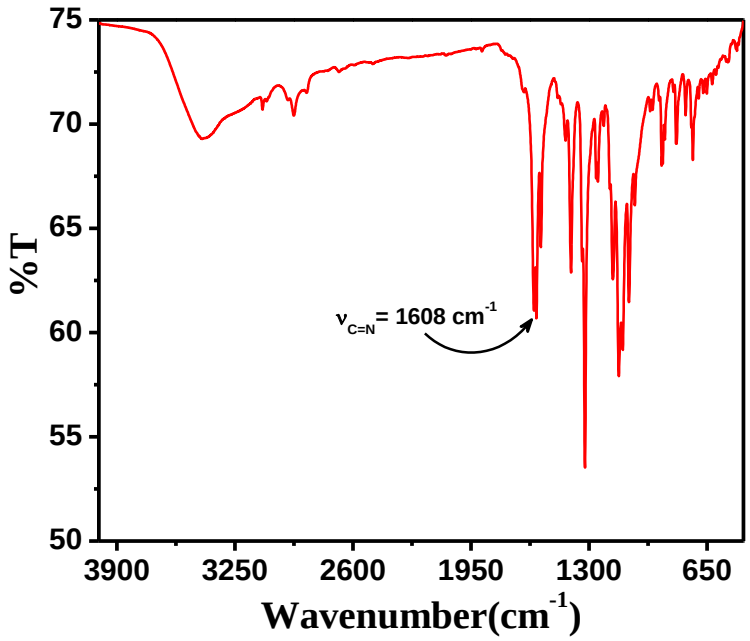

Figure S12: FTIR Spectrum of ^{Me}**L4** in KBr disk, in the range 4000-400 cm^{-1}.

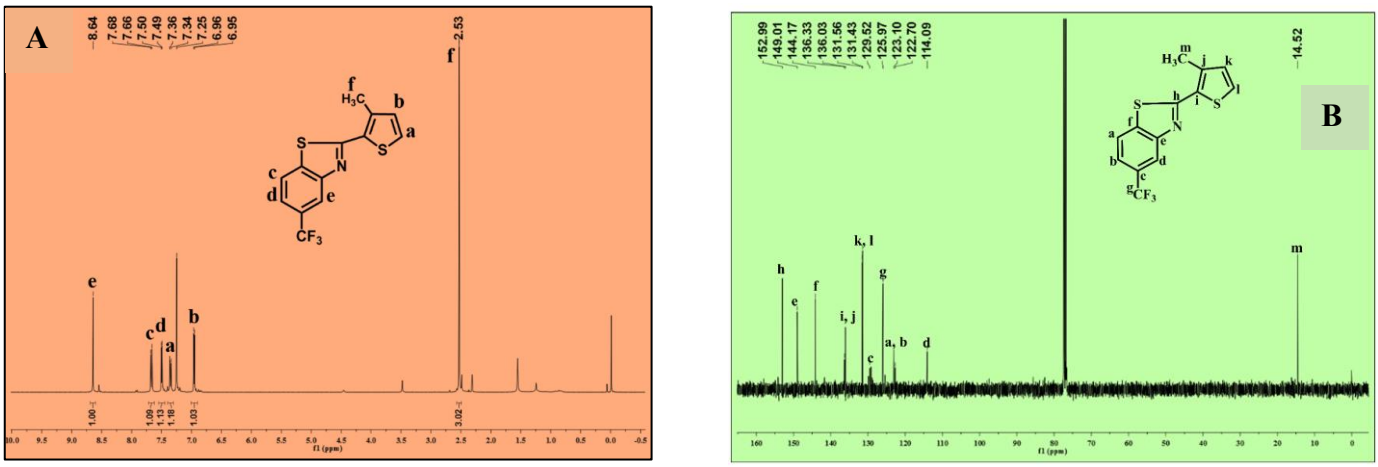

Figure S13: (A) ^{1}H NMR spectrum of ^{Me}**L4** in $CDCl_3$, **(B)** ^{13}C-NMR spectrum of ^{Me}**L4** in $CDCl_3$.

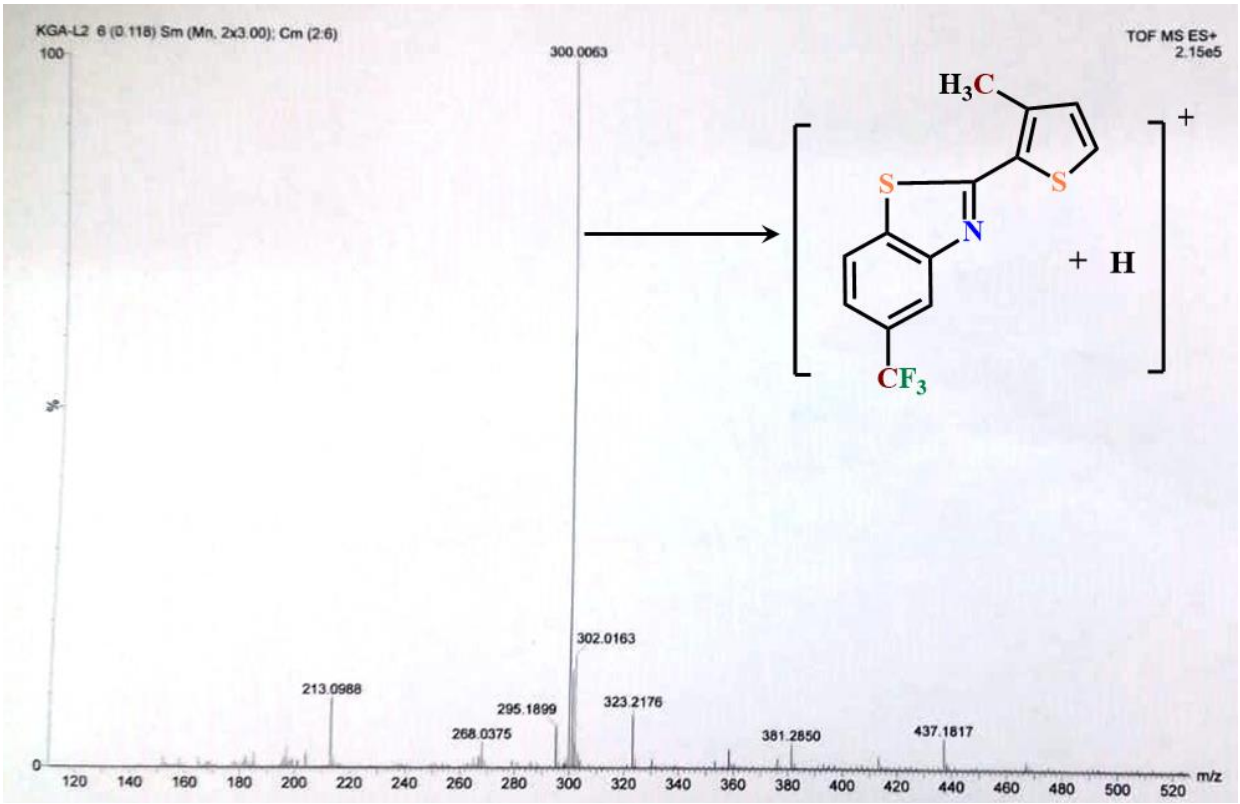

Figure S14: ESI mass spectrum of ^{Me}**L4** measured in CH_2Cl_2, peak at *m/z* = 300.006 corresponds to $\{M+H\}^+$.

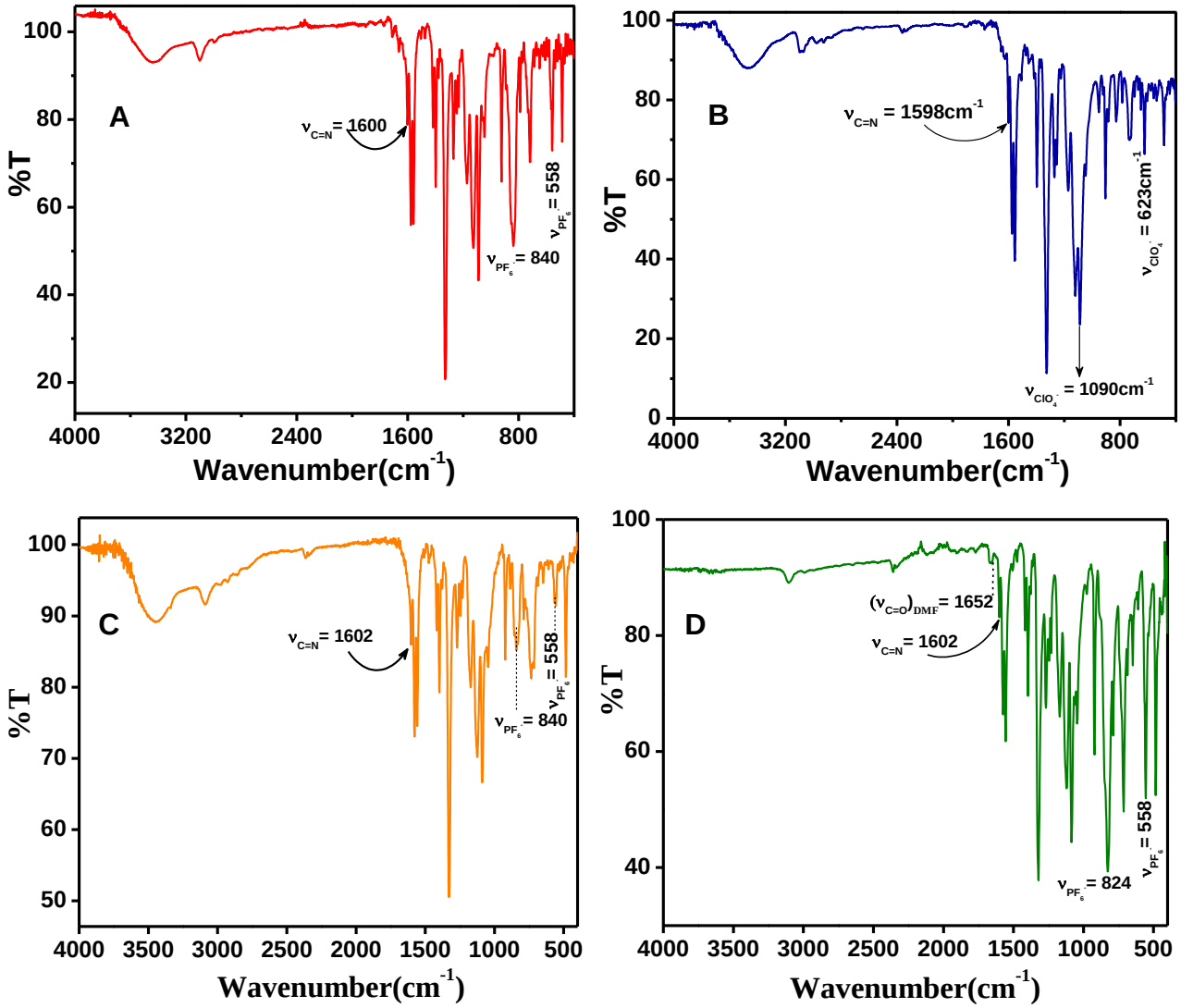

Figure S15: (A) FT-IR spectrum of **1**(red) in KBr disk, in the range 4000-400 cm^{-1}, **(B)** FTIR Spectrum of **2**(blue) in KBr disk, in the range 4000-400 cm^{-1}, **(C)** FTIR Spectrum of **3**(orange) in KBr disk, in the range 4000-400 cm^{-1}, **(D)** FT-IR spectrum of **3**(olive) in ATR mode, in the range 4000-400 cm^{-1}.

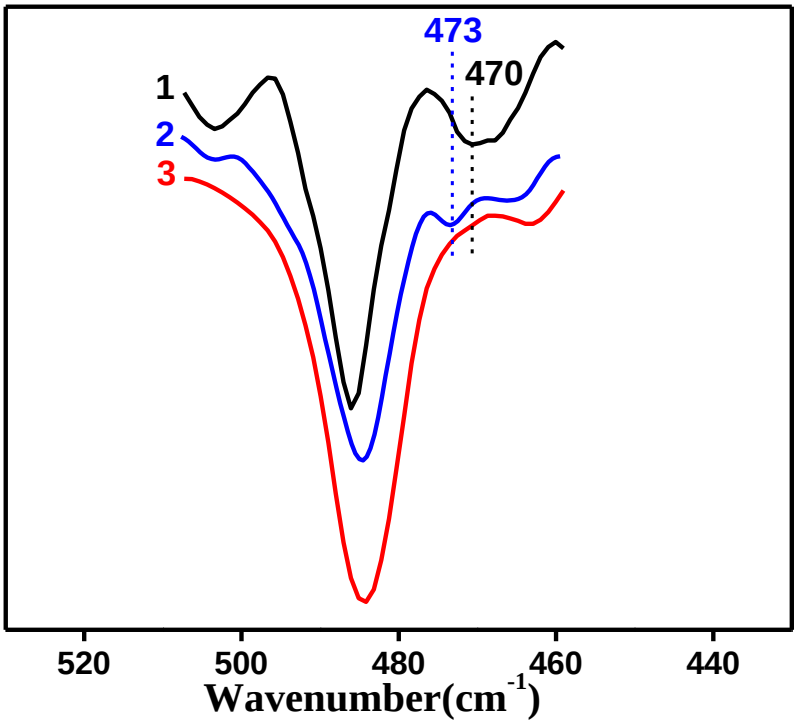

Figure S16: FT-IR spectra of **1**(black), **2**(blue) and **3**(red) measured in KBr disk, showing $\nu_{Cu\text{-}S}{}^{s}$ at 470cm^{-1} for **1** (dotted black vertical line) and 473cm^{-1} for **2** (dotted blue vertical line) and is absent from **3**.

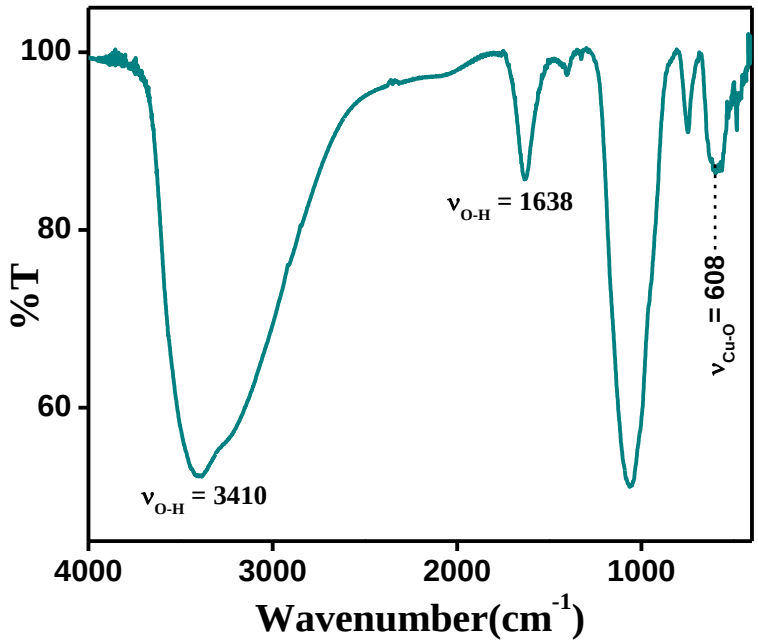

Figure S17: FT-IR spectrum of the green compound obtained while formation of **3** from **1**, in KBr disk, in the range 4000-400 cm^{-1}.

EDAX APEX

kV: 20	Mag:1000	Takeoff: 33.6	Live Time(s): 204.8	Amp Time(µs): 0.96	Resolution(eV)128.9

Sum Spectrum

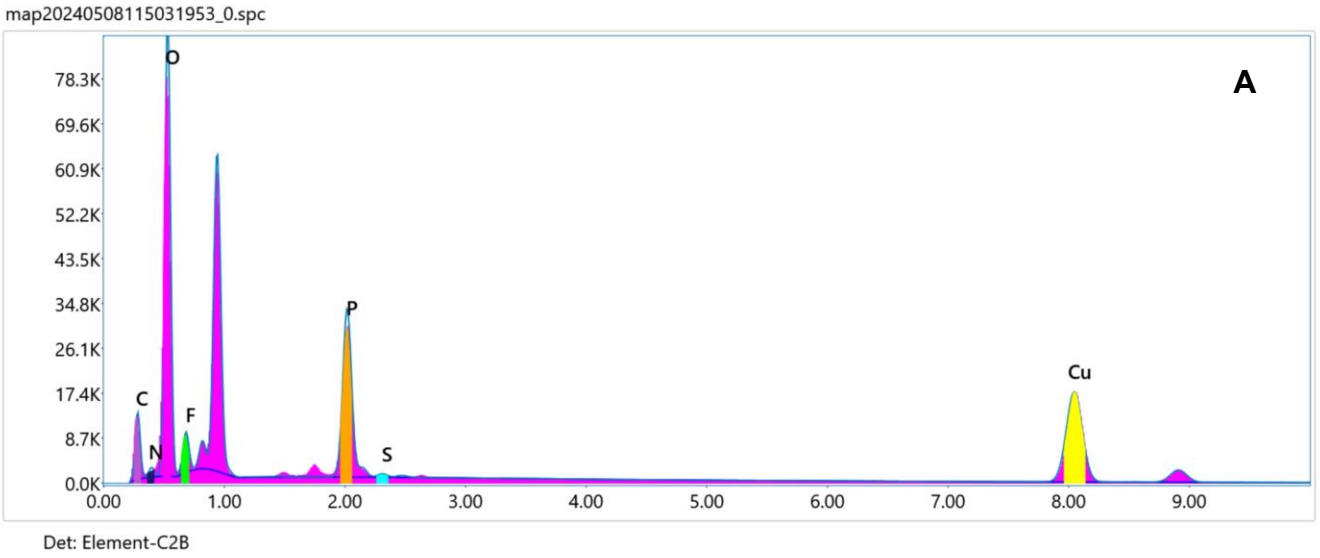

B

Smart Quant Results

Element	Weight %	Atomic %	Net Int.	Error %	R	A	F
C K	16.7	27.9	333.7	10.9	0.8822	0.0584	1.0000
N K	2.0	2.8	49.9	12.7	0.8889	0.0733	1.0000
O K	39.9	49.9	2580.6	9.6	0.8944	0.1489	1.0000
F K	5.0	5.2	239.5	10.7	0.8994	0.1005	1.0000
P K	8.3	5.4	1418.3	5.1	0.9244	0.6099	1.0078
S K	0.2	0.1	28.6	9.8	0.9279	0.6583	1.0114
CuK	27.9	8.8	1383.8	2.2	0.9666	0.9894	1.0586

Figure S18: EDS spectrum of green amorphous compound obtained while formation of **3** from **1, (A)** Sum spectrum**, (B)** tabulated smart quant results.

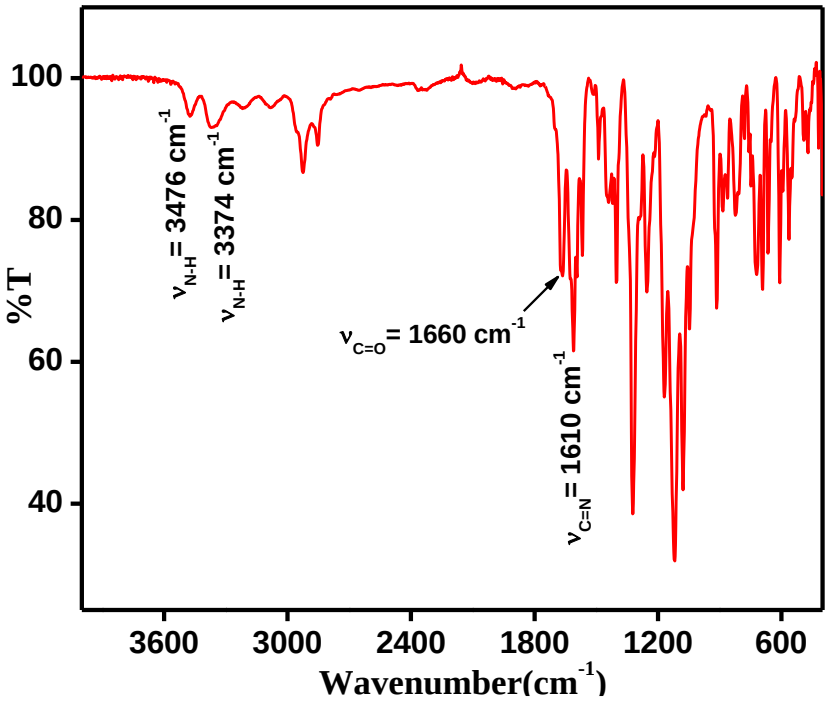

Figure S19: ATR mode FTIR Spectrum (4000-400 cm^{-1}) of the semisolid isolated from the mother liquor (DMF/toluene) of conversion **1→3** + CuO (mother liquor was evaporated at 60 ^{0}C temperature under vacuum, next extracted with $CHCl_3$ and evaporated again to get this semisolid).

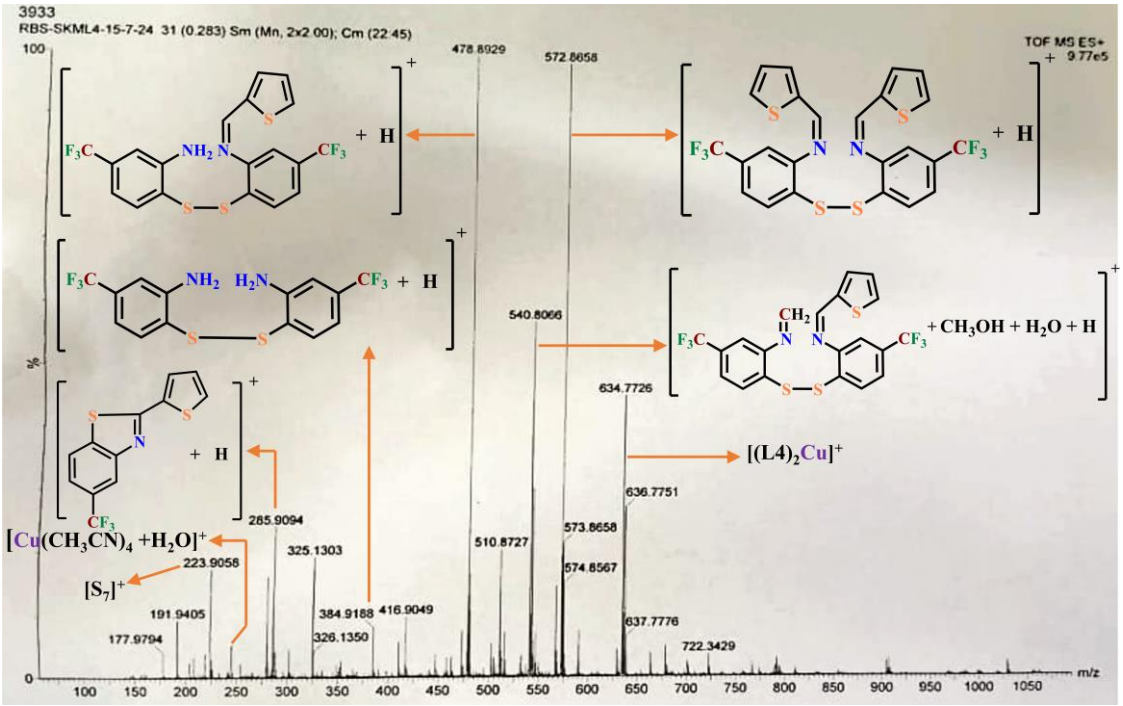

Figure S20: ESI mass spectrum of the semisolid isolated from the mother liquor (DMF/toluene) of conversion **1→3** + CuO (mother liquor was evaporated at 60 ^{0}C temperature under vacuum, next extracted with $CHCl_3$ and evaporated again to get this semisolid).

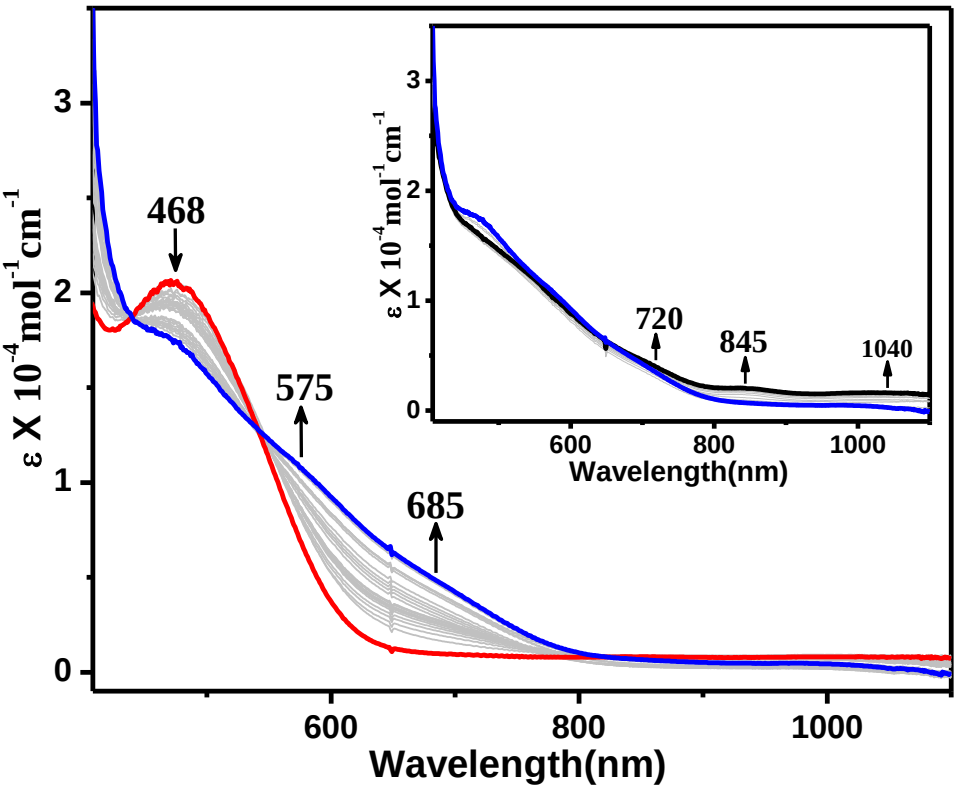

Figure S21: UV-Vis spectral changes of **3** in DMF upon addition of 1.5 equivalent of Na_2S dissolving in 100µL of CH_3OH. [**3**] = 10^{-4} M. Red trace is for **3**, grey traces are recorded in a time interval of 4 minute and blue is the final trace; Inset: UV-Vis spectral changes of the same solution recorded with 30 minute time interval starting from the same blue trace of the main Figure to the final black trace indicating conversion of **3**→**1**^{Red}→**1** i.e. red→blue→black trace.

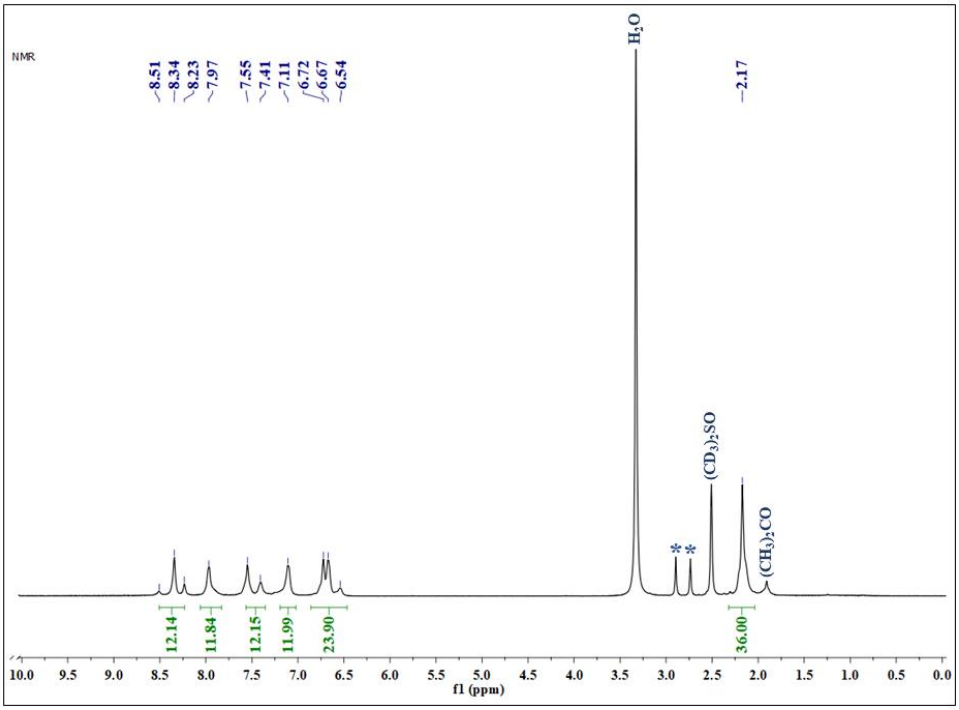

Figure S22: ^{1}H NMR spectrum of **2** in d_6-dmso at 298K. DMF(asterisked), Acetone are present as impurities.

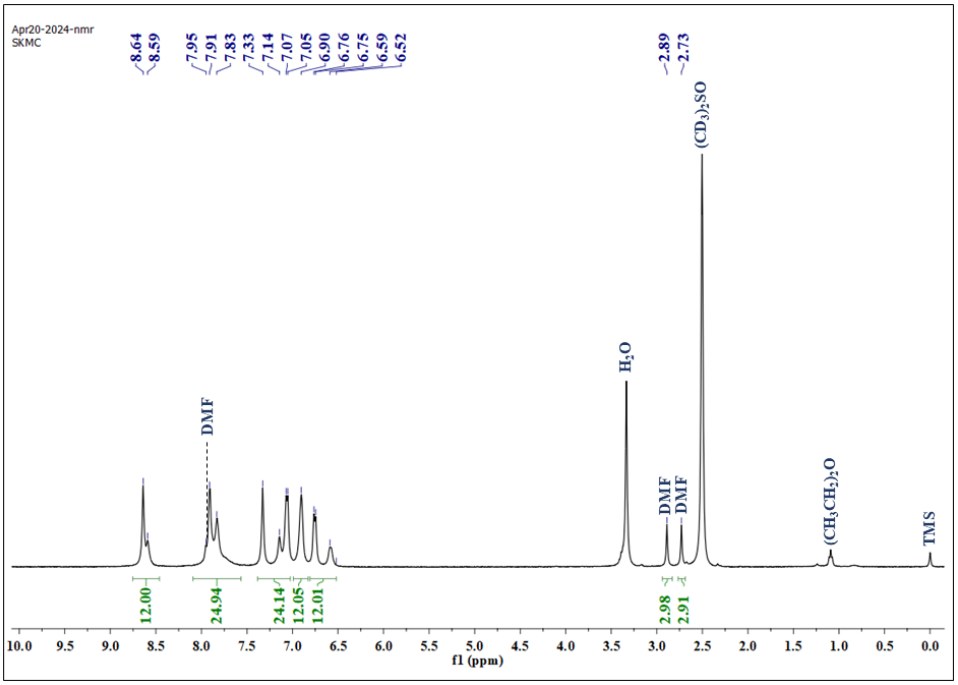

Figure S23: ^{1}H NMR spectrum of **3** in d_6-dmso at 298 K. Peak positions for coordinated DMF molecule are also shown. Diethyl ether is present as impurity.

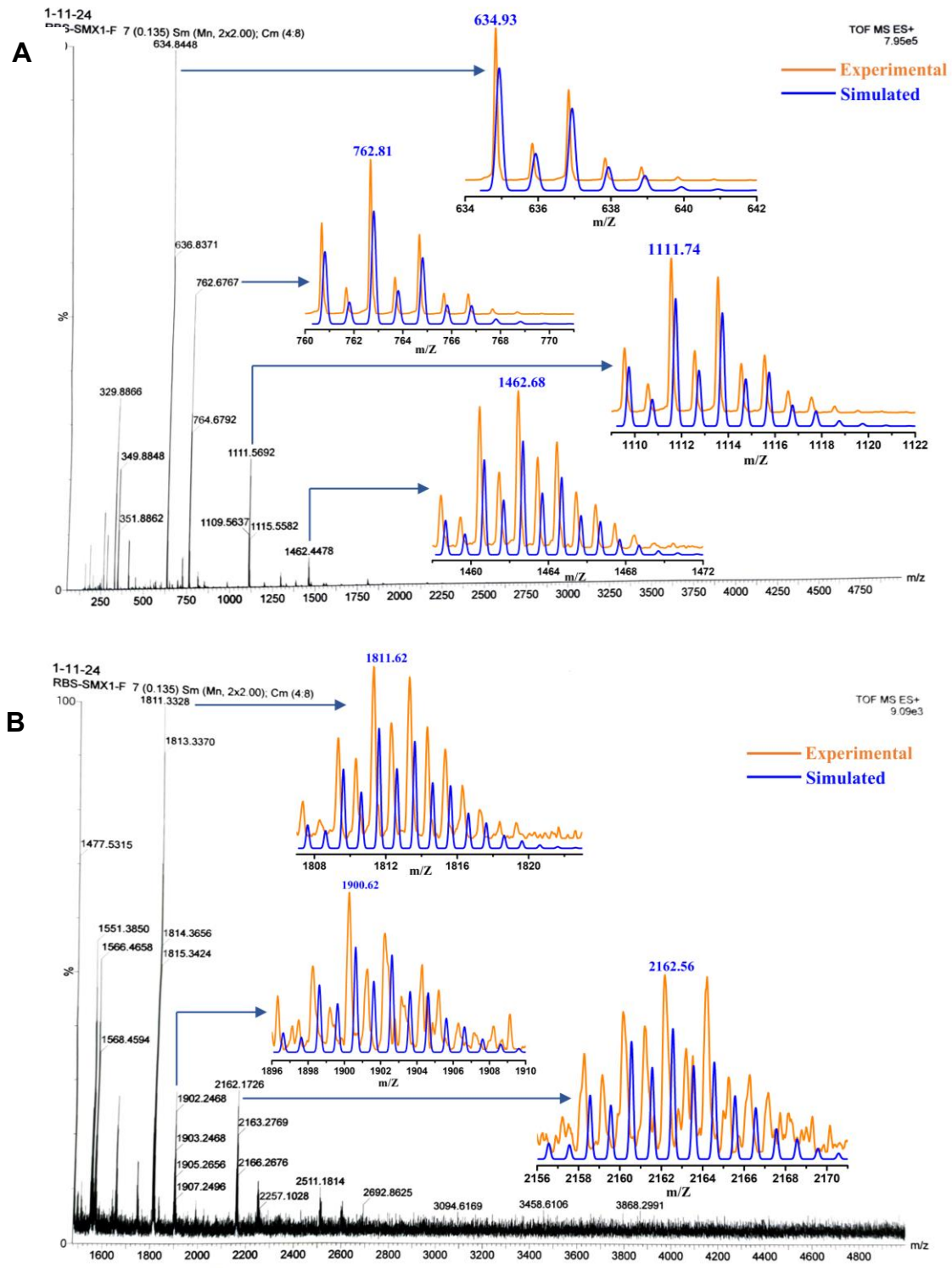

Figure S24: ESI positive mass spectrum of **1** measured in CH_3OH, (A) peaks at m/z = 634.84, 762.67, 1111.56 and 1462.44, correspond to $[(L4)_2Cu]^+$, $[(L4)_2Cu_3]^+$, $[(L4)_3Cu_4]^+$ and $[(L4)_4Cu_5]^+$ respectively; (B) peaks at 1811.33, 1900.24 and 2162.17 correspond to $[(L4)_5Cu_6]^+$, $[(L4)_5Cu_6 + CH_3OH + H_2O + K]^+$ and $[(L4)_6Cu_7]^+$ respectively.

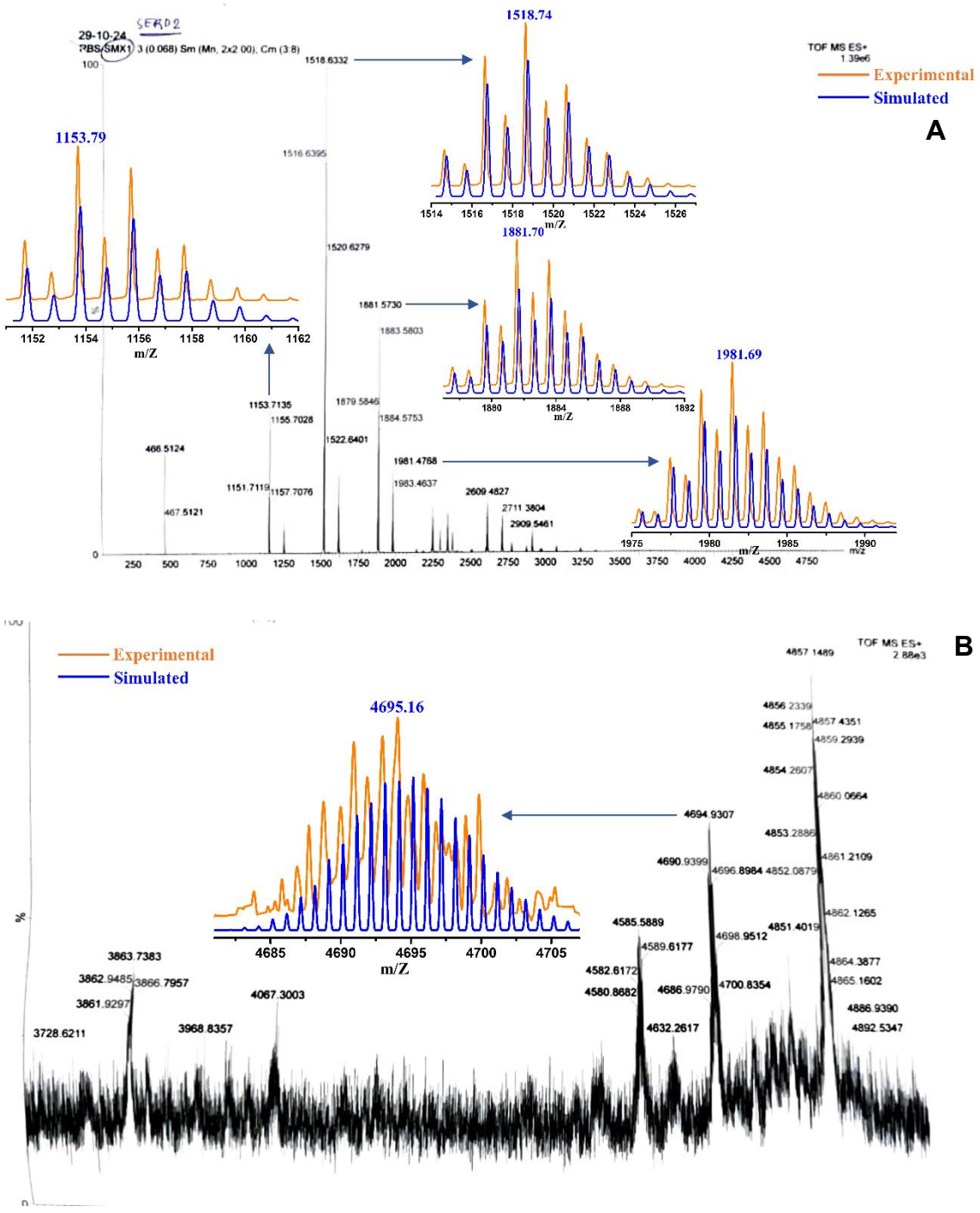

Figure S25: ESI positive mass spectrum of **2** measured in CH_3OH ; (**A**) peaks at m/z = 1153.71, 1518.63, 1881.57 and 1981.47 correspond to $[(^{Me}L4)_3Cu_4]^+$, $[(^{Me}L4)_4Cu_5]^+$, $[(^{Me}L4)_5Cu_6]^+$ and $[(^{Me}L4)_5Cu_7+CH_3OH+3H]^+$ respectively, (**B**) peaks at m/z = 4694.93 corresponds to $\{[(^{Me}L4)_{12}Cu_{16}(\mu_4\text{-}S)]+H_2O+H+Na\}^+$.

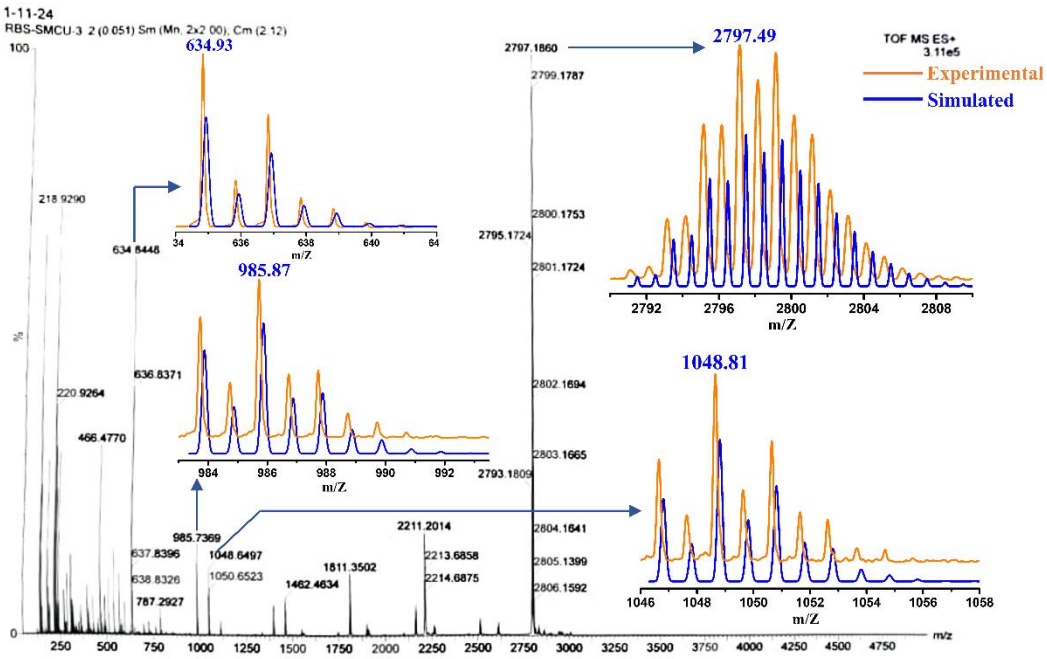

Figure S26: ESI positive mass spectrum of **3** measured in CH_3OH, peaks at m/z = 634.84, 985.87, 1048.64, and 2797.18 correspond to $[(L4)_2Cu]^+$, $[(L4)_3Cu_2]^+$, $[(L4)_3Cu_3]^+$ and $[(L4)_8Cu_8]^+$ respectively.

The ESI mass spectra of **1**-**3** have been measured second time considering crystals obtained following different batch of syntheses that also displays no molecular ion peak but the similar type fragmented pattern those correspond to the mass of various species with different metal-ligand combinations. These ESI mass spectra of the clusters **1**-**3** are shown below.

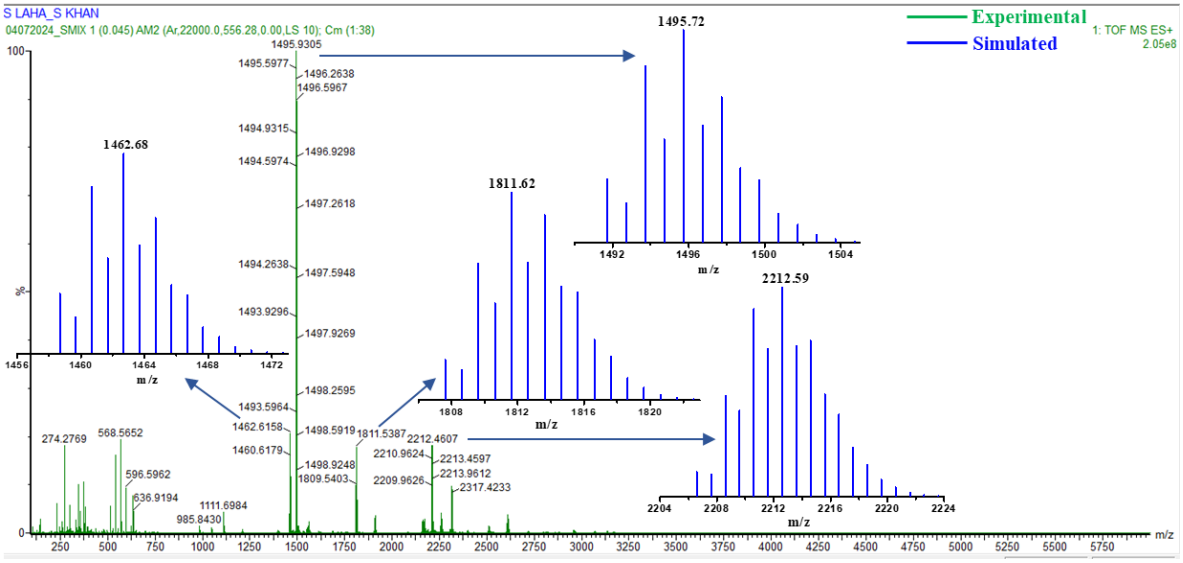

ESI positive mass spectrum of **1** measured in CH_3OH, peaks at m/z = 1462.61, 1495.93, 1811.62 and 2212.46 correspond to $[(L4)_4Cu_5]^+$, $[(L4)_4Cu_5+CH_3OH+H]^+$, $[(L4)_5Cu_6]^+$ and $[(L4)_6Cu_7+CH_3OH+H_2O]^+$ respectively.

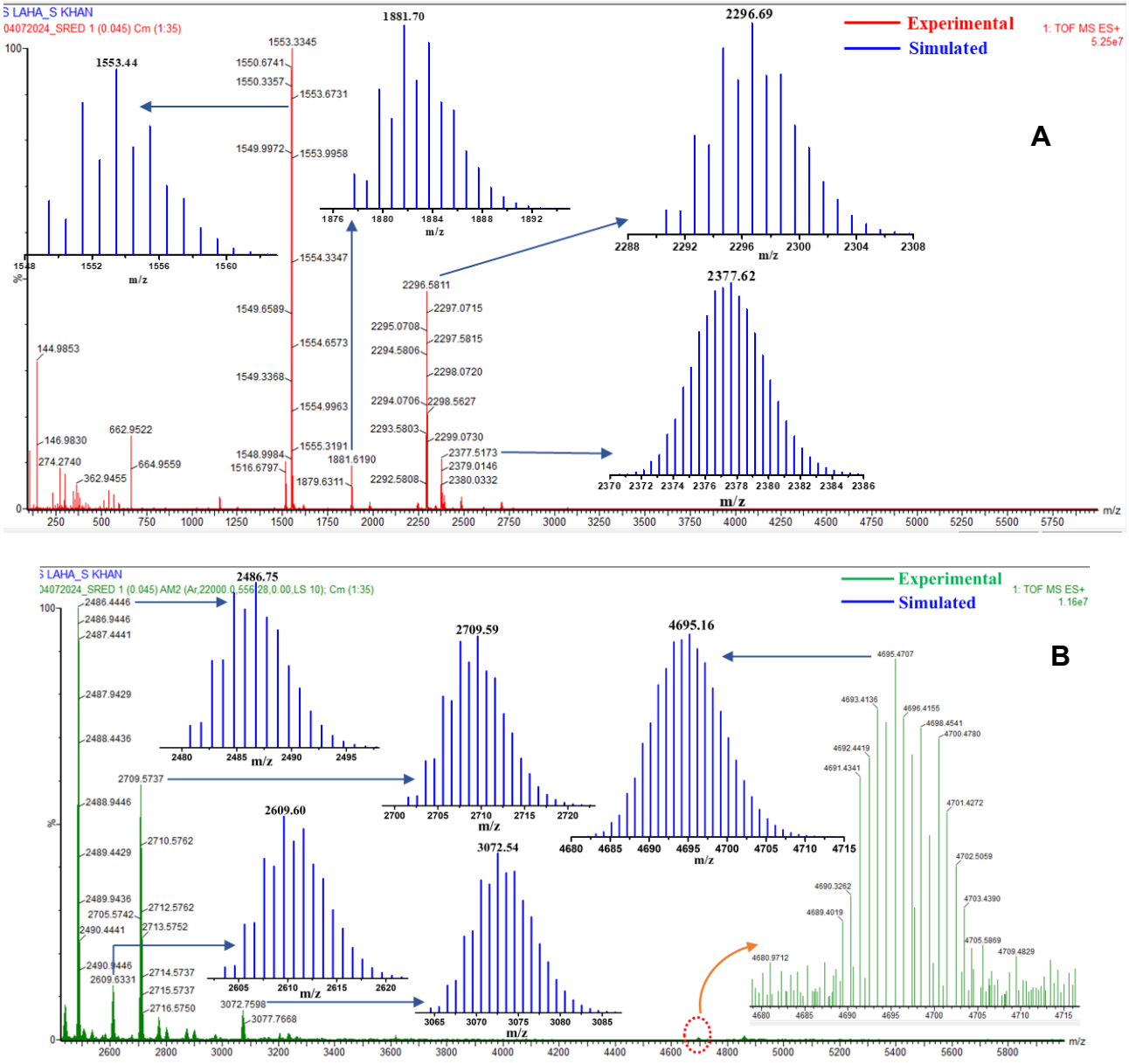

ESI positive mass spectrum of **2** measured in CH_3OH; (**A**) peaks at m/z = 1553.33, 1881.61, 2296.58 and 2377.51 correspond to $[(^{Me}L4)_4Cu_5+CH_3OH+3H]^+$, $[(^{Me}L4)_5Cu_6]^+$, $[(^{Me}L4)_6Cu_7+CH_3OH+H_2O]^+$ and $\{[(^{Me}L4)_{12}Cu_{16}(\mu_4\text{-}S)]+2CH_3OH+2H_2O+2H\}^{2+}$ respectively, (**B**) peaks at m/z = 2486.44, 2609.63, 2709.57 and 3072.75 correspond to $[(^{Me}L4)_7Cu_6+3H]^+$, $[(^{Me}L4)_7Cu_8]^+$, $[(^{Me}L4)_7Cu_9+CH_3OH+3H]^+$ and $[(^{Me}L4)_8Cu_{10}+CH_3OH+3H]^+$ respectively; In the magnified vision the peak at m/z = 4695.47 corresponds to $\{[(^{Me}L4)_{12}Cu_{16}(\mu_4\text{-}S)]+H_2O+H+Na\}^+$.

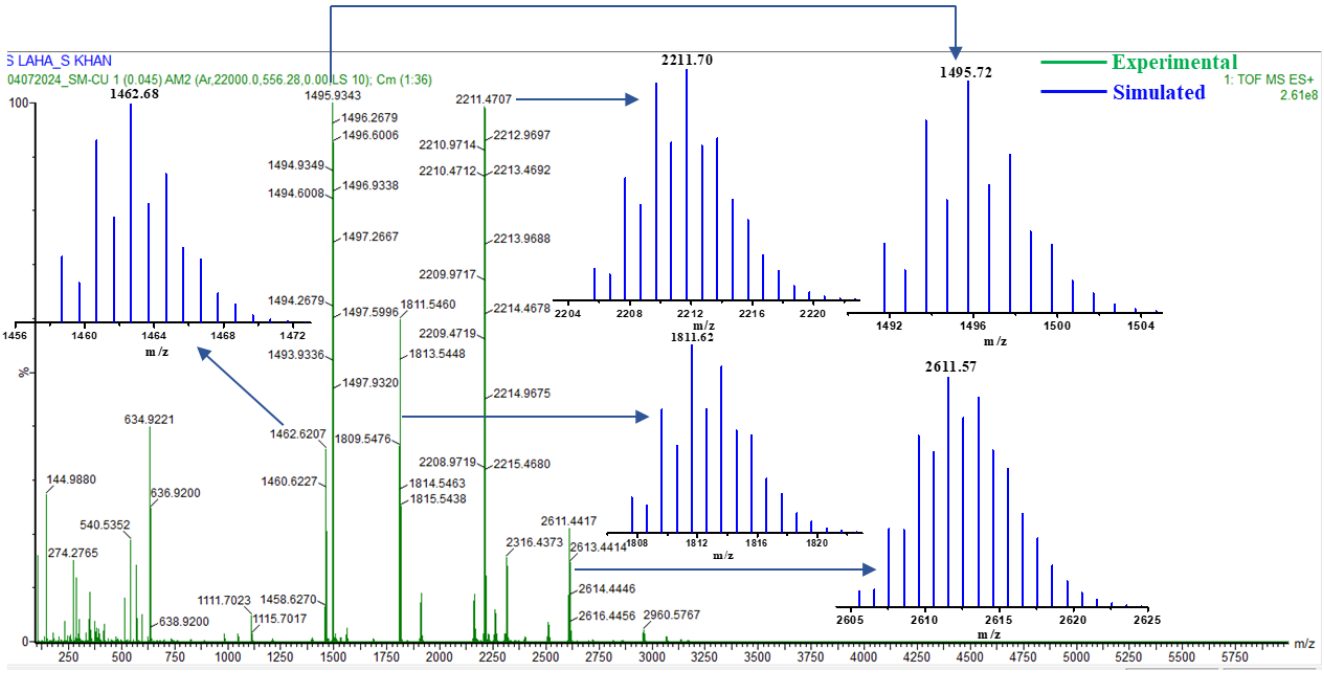

ESI positive mass spectrum of **3** measured in CH_3OH, peaks at m/z = 1462.62, 1495.93, 1811.54, 2211.47 and 2611.44 correspond to $[(L4)_4Cu_5]^+$, $[(L4)_4Cu_5+CH_3OH+H]^+$, $[(L4)_5Cu_6]^+$, $\{(L4)_5Cu_6+[Cu(CH_3OH)_6]PF_4+2H_2O\}^+$ and $[(L4)_7Cu_8+2CH_3OH+2H_2O]^+$ respectively.

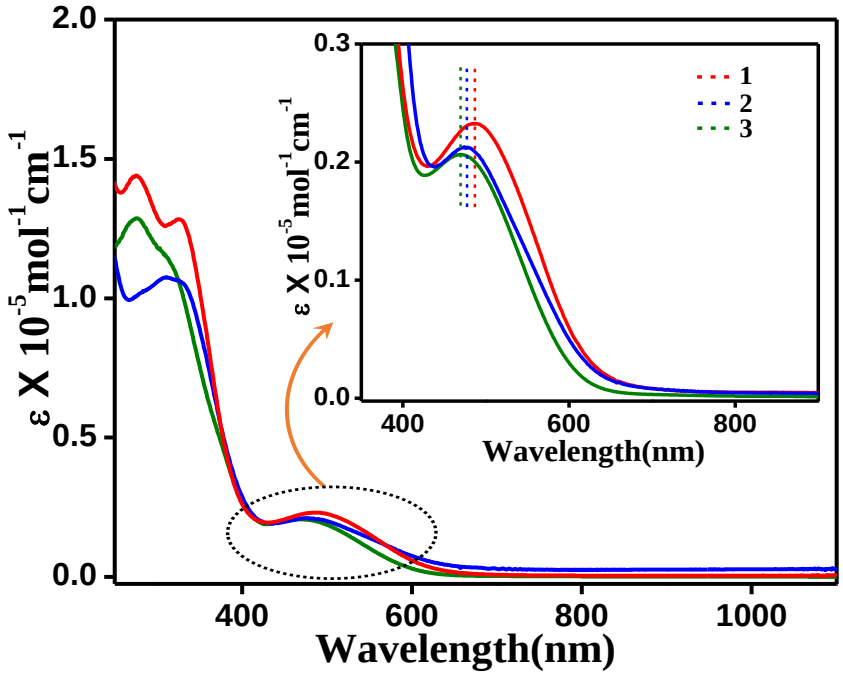

Figure S27: UV-Vis spectra of the CH_3CN solution of **1** (red), **2** (blue) and **3** (green), measured at 298K; inset: magnified vision (x 10) of the spectra in the range 350-850 nm showing the shift of thiolato-$S^- \rightarrow Cu^{x+}$ (avg. x = +1.062, +0.937 and +0.882 for **1**-**3** respectively) charge transfer band.

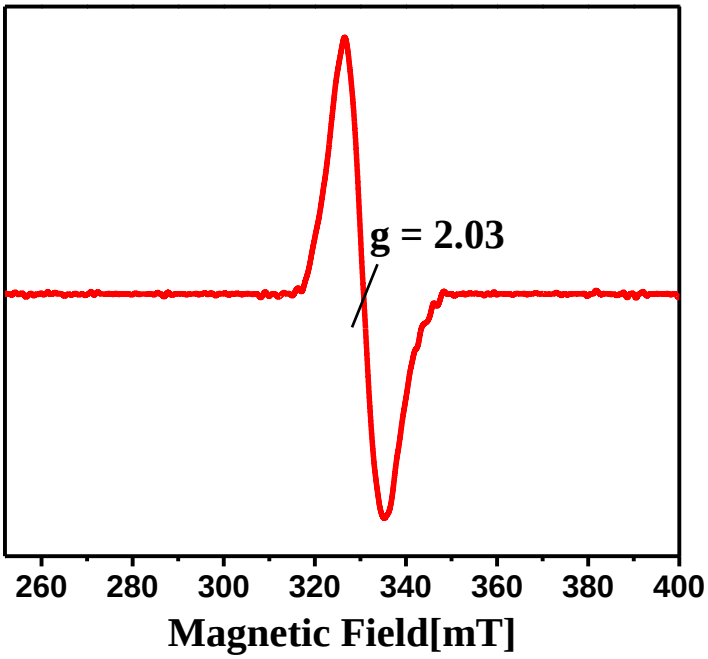

Figure S28: X-Band EPR spectrum of **1** in CH_3OH at 77K. Spectrometer settings: microwave frequency = 9.416 GHz, power = 10mW, modulation frequency = 100 kHz and modulation amplitude = 5 G.

EDAX APEX of 1

kV:	Mag:	Takeoff:	Live Time(s):	Amp Time(µs):	Resolution:(eV)
20	1500	33.6	204.8	0.96	128.9

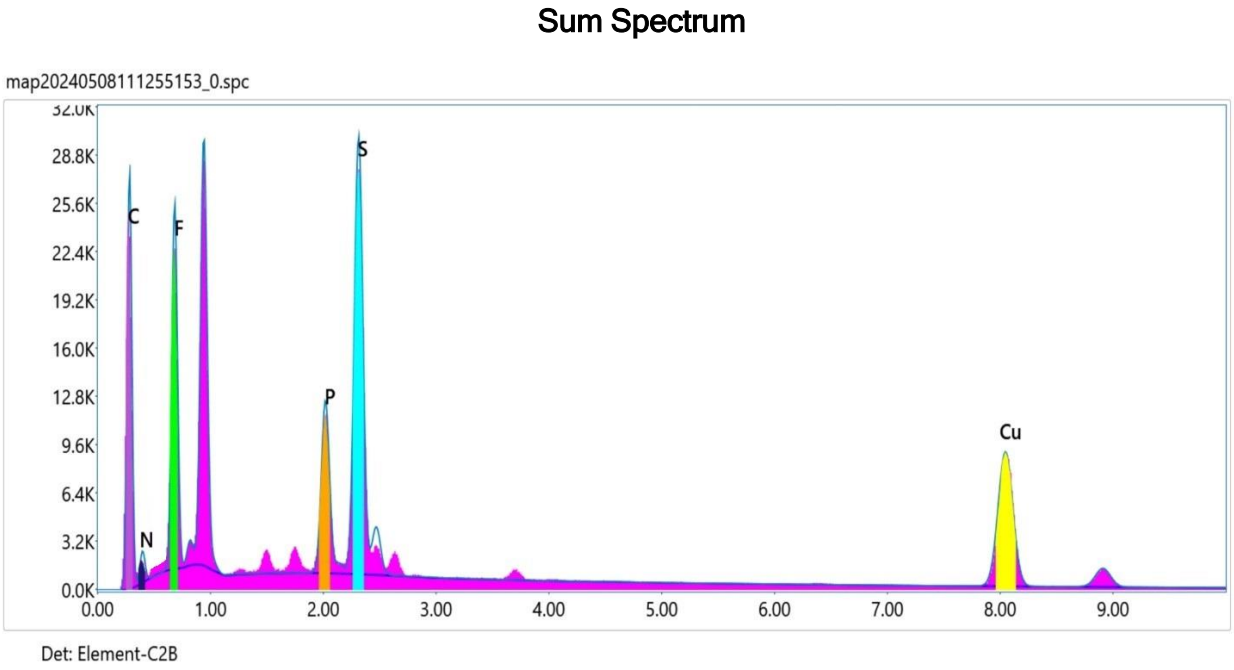

Figure S29: EDS spectrum of **1**, indicating the presence of C, N, F, P, S and Cu.

EDAX APEX of 2

kV:	Mag:	Takeoff:	Live Time(s):	Amp Time(µs):	Resolution:(eV)
20	1500	34	204.8	0.96	128.9

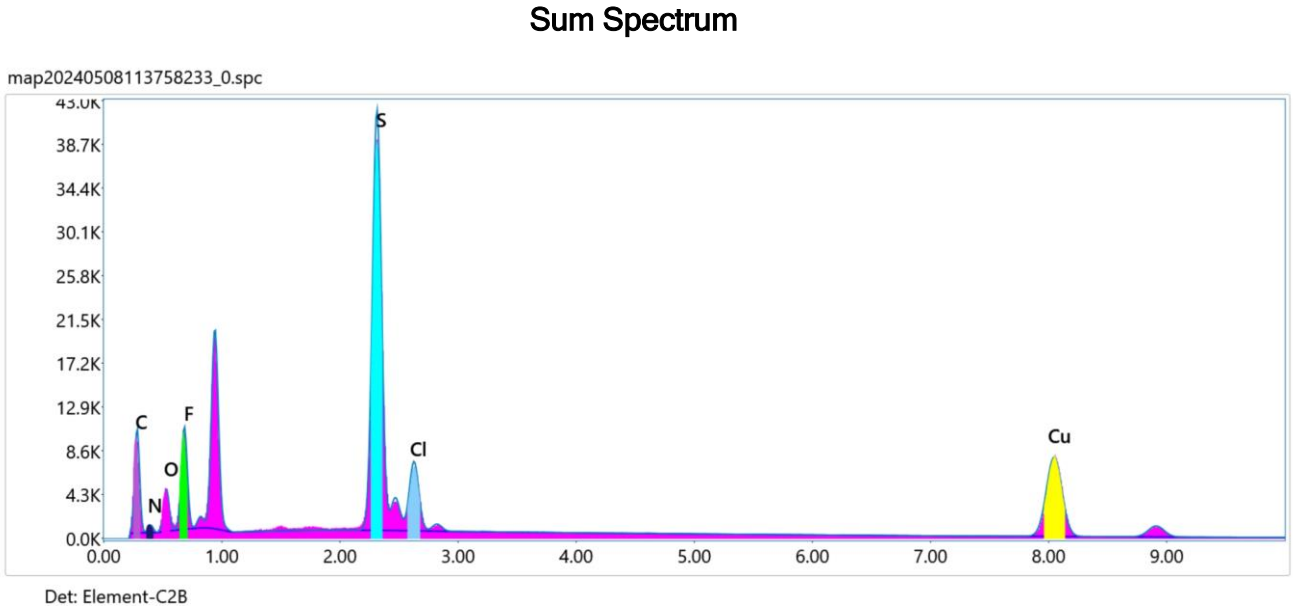

Figure S30: EDS spectrum of **2**, indicating the presence of C, N, O, F, S, Cl and Cu.

EDAX APEX of 3

kV: 20	Mag:1000	Takeoff: 33.5	Live Time(s): 204.8	Amp Time(µs): 0.96	Resolution:(eV)128.9

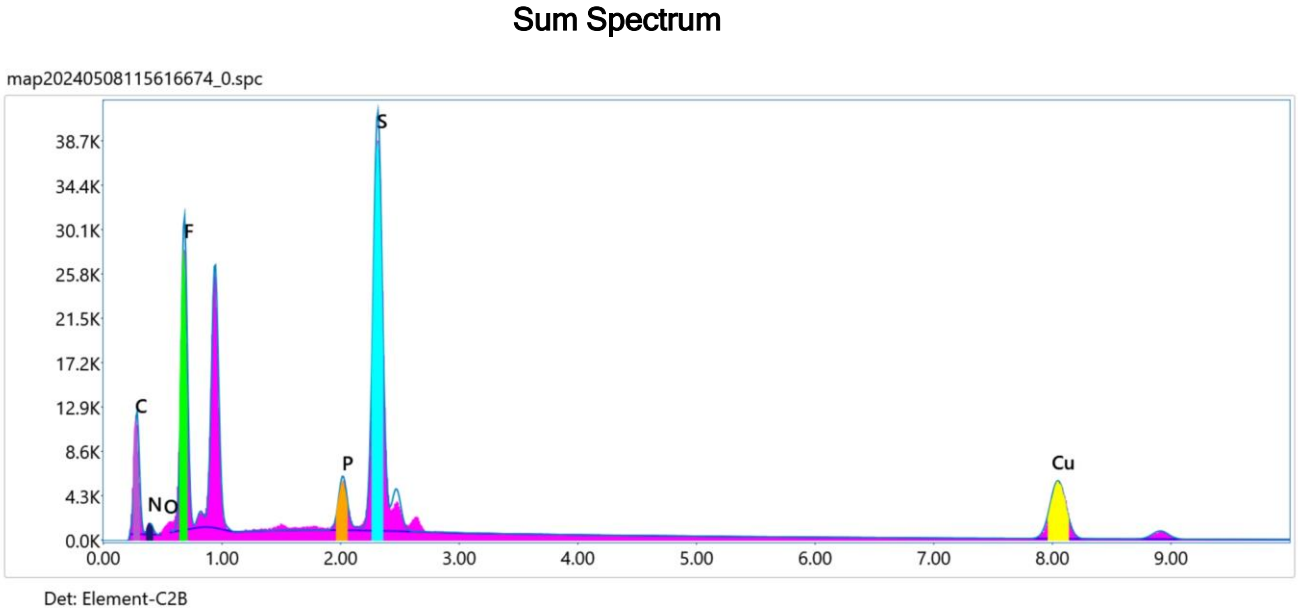

Figure S31: EDS spectrum of **3**, indicating the presence of C, N, O, P, S and Cu.

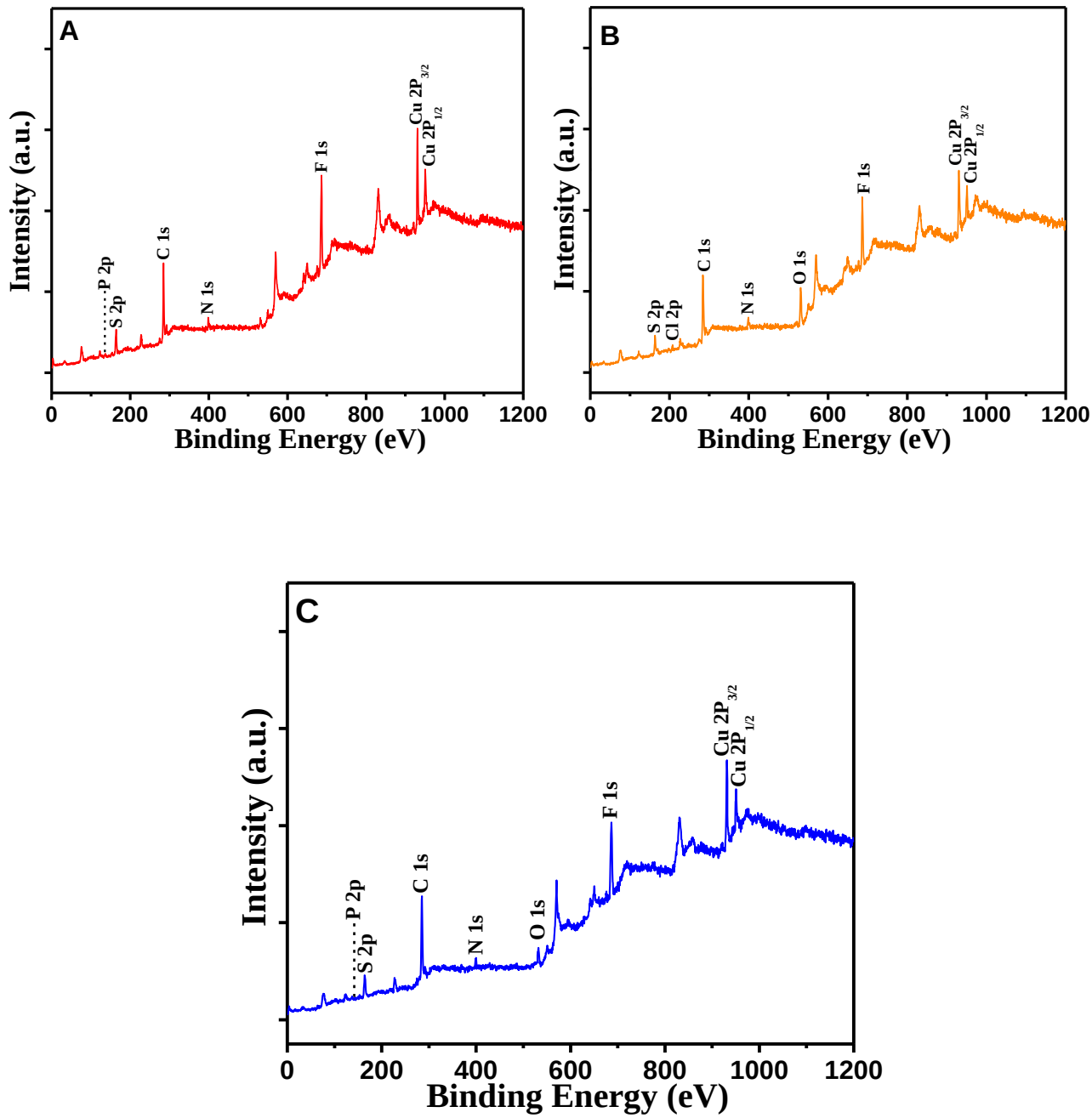

Figure S32: XPS survey spectra of **1**(A), **2**(B) and **3**(C) confirming the presence of Cu, S, P, C, N, F in **1**, Cu, S, Cl, C, N, O, F in **2** and Cu, S, P, C, N, O, F in **3**.

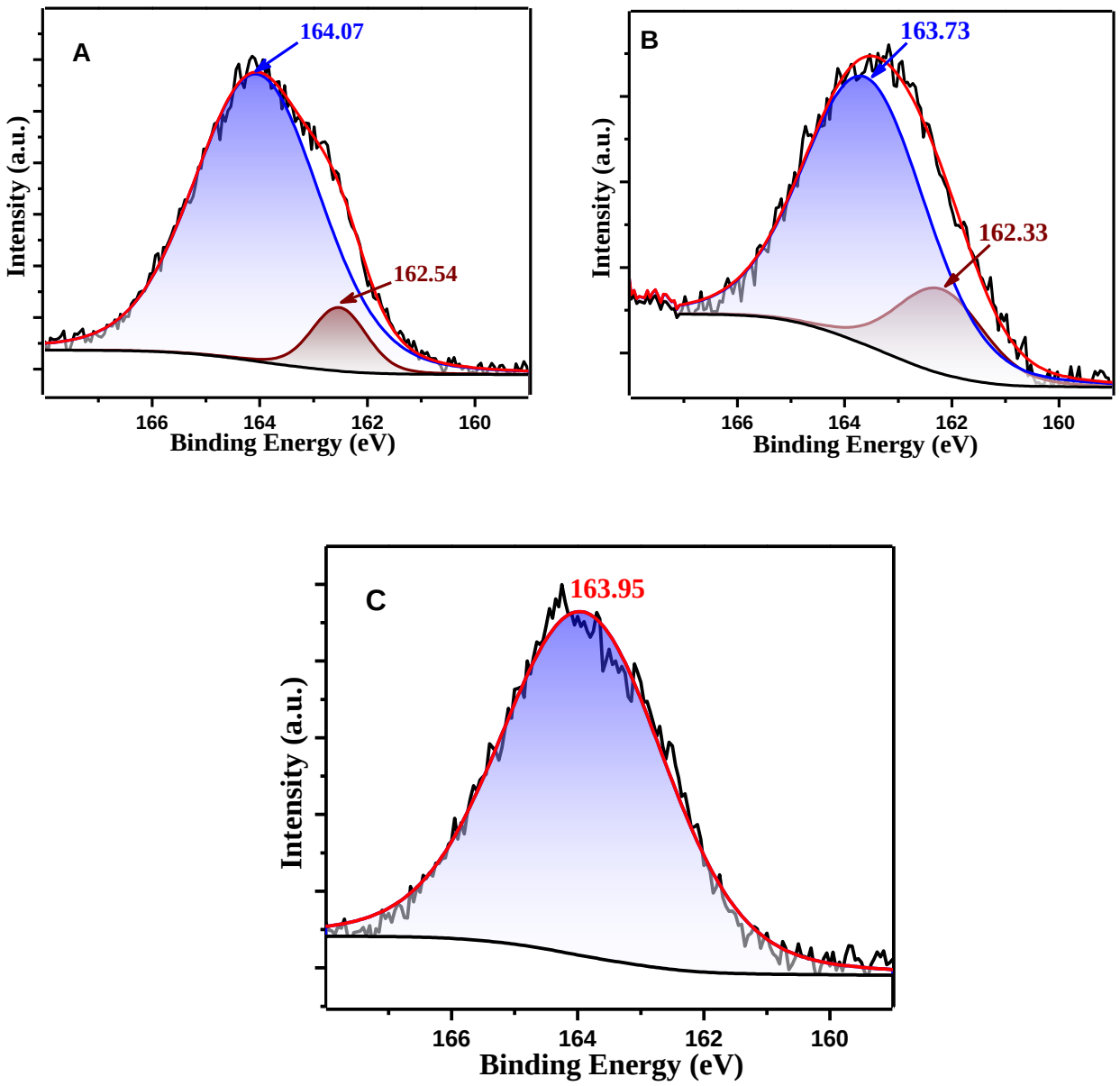

Figure S33: High resolution XPS spectra of **1**(A), **2**(B) and **3**(C) showing the S 2p region. For **1** and **2** the peaks have been deconvoluted into two peaks (for thiolato-S and sulfido-S), the positions of the peaks are shown in the diagrams.

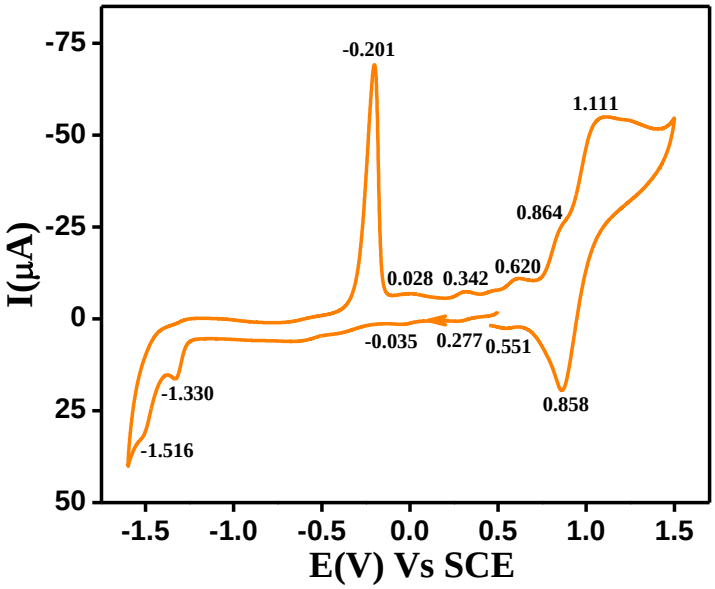

Figure S34: Cyclic voltammogram of **1** in CH_3CN containing 0.1 M $[(n\text{-}Bu)_4N]ClO_4$ as a supporting electrolyte at 298 K at a platinum working electrode using SCE as reference electrode at a scan rate 50 mV s^{-1}.

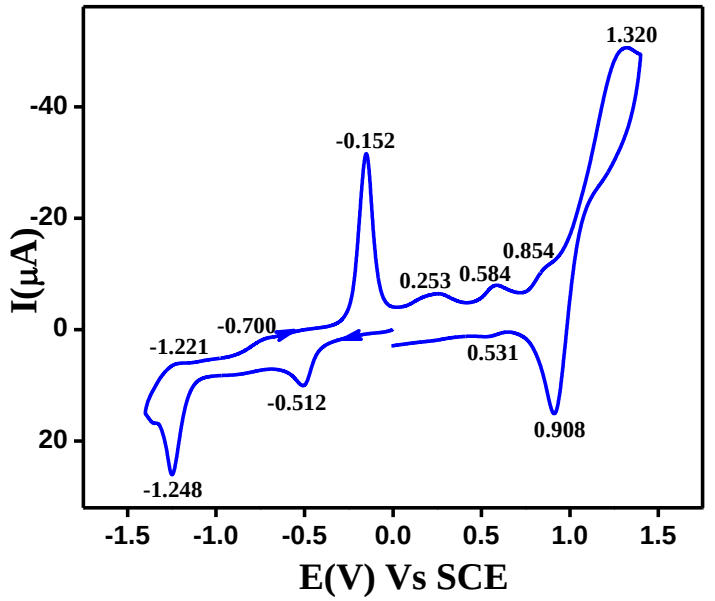

Figure S35: Cyclic voltammogram of **2** in CH_3CN containing 0.1 M $[(n\text{-}Bu)_4N]ClO_4$ as a supporting electrolyte at 298 K at a platinum working electrode using SCE as reference electrode at a scan rate 50mVs^{-1}.

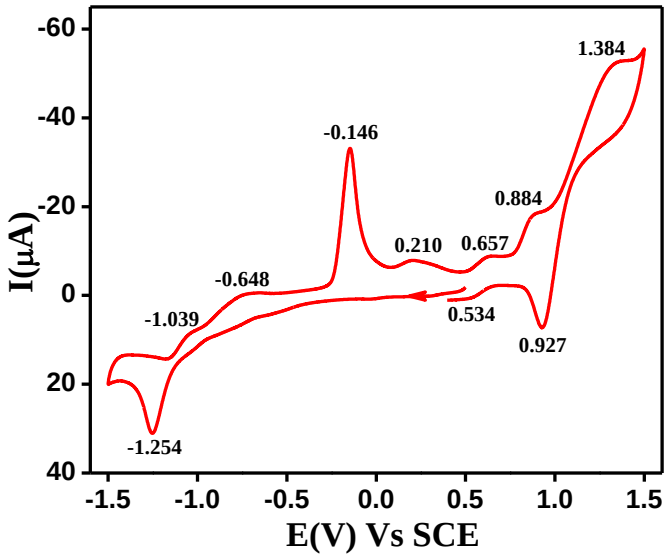

Figure S36: Cyclic voltammogram of **3** in CH_3CN containing 0.1 M $[(n\text{-}Bu)_4N]ClO_4$ as a supporting electrolyte at 298 K at a platinum working electrode using SCE as reference electrode at a scan rate 50mVs^{-1}.

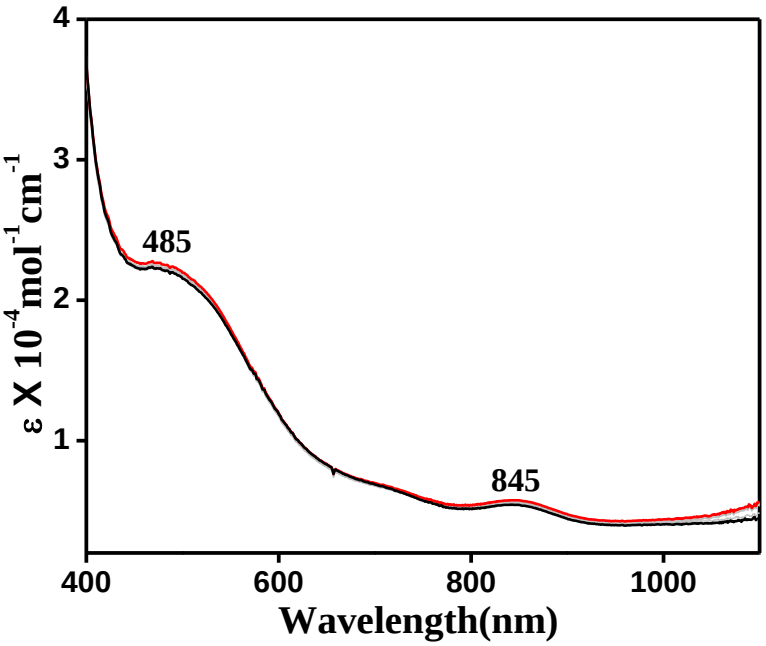

Figure S37: UV-Vis spectral changes upon electrolysis of **1** in CH_3CN at an applied potential of +0.12V at 298K; black- initial spectrum and red- final spectrum.

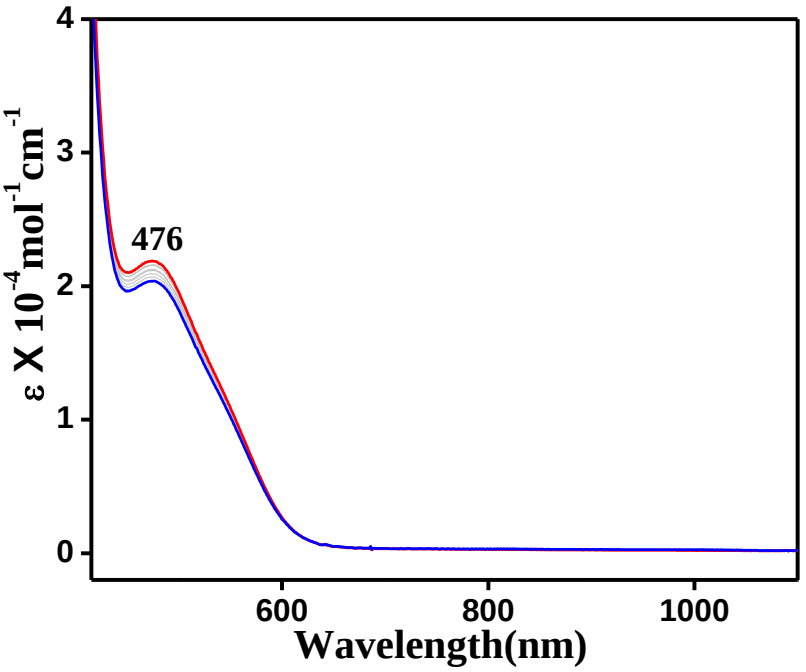

Figure S38: UV-Vis spectral changes upon electrolysis of **2** in CH_3CN at an applied potential of -0.15 V at 298 K; red- initial spectrum and blue- final spectrum.

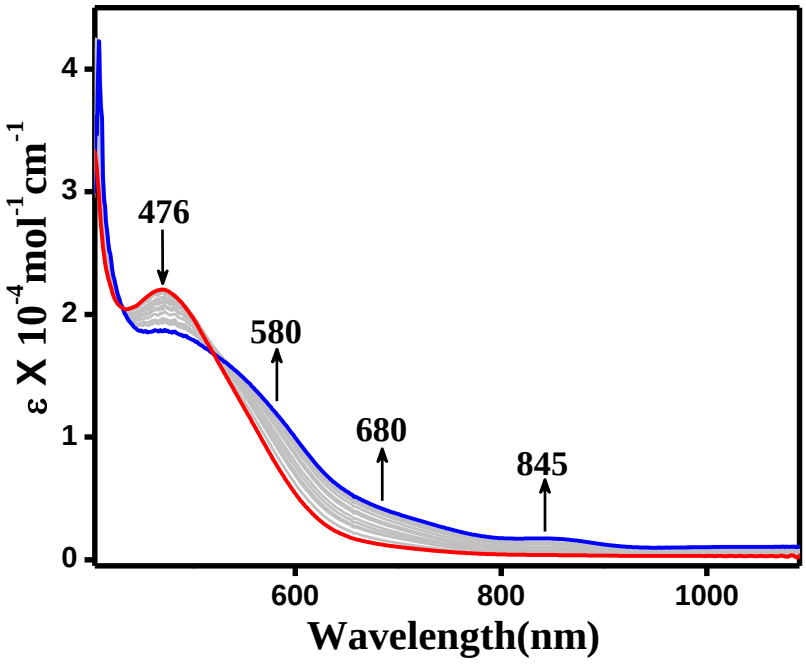

Figure S39: UV-Vis spectral changes upon one electron oxidation of **2** in CH_3CN at an applied potential of +0.07V at 298K showing conversion of **2**(red) → $\mathbf{2^{ox}}$(blue), **[2]** = 10^{-4} M.

References:

1. W. R. Robinson, *J. Chem. Educ.*, 1985, **62**, 1001.

2. G. M. Sheldrick, *Acta Crystallogr. Sect. A.*, 2015, **71**, 3-8.

3. G. M. Sheldrick, *Acta Crystallogr. Sect. C*: *Struct. Chem.*, 2015, **C71**, 3-8.

4. O. V. Dolomanov, L. J. Bourhis, R. J. Gildea, A. K. Howard and H. Puschmann, *J. Appl. Cryst.*, 2009, **42**, 339-341.

5. C. F. Macrae, I. Sovago, S. J. Cottrell, P. T. A. Galek, P. McCabe, E. Pidcock, M. Platings, G. P. Shields, J. S. Stevens, M. Towler and P. A. Wood, *J. Appl. Cryst.*, 2020, **53**, 226-235.